Build-up and depositional dynamics of an arc front volcaniclastic complex: the Miocene Tepoztlán Formation (Transmexican Volcanic Belt, Central Mexico)

Nils Lenhardt[a,d*], Jens Hornung[a], Matthias Hinderer[a], Harald Böhnel[b], Ignacio S. Torres-Alvarado[c] and Nico Trauth[a]

[a]Institut für Angewandte Geowissenschaften, Technische Universität Darmstadt, Darmstadt, Germany

[b]Centro de Geociencias, Universidad Nacional Autónoma de México, Queretaro, Mexico

[c]Centro de Investigacíones en Energía, Universidad Nacional Autónoma de México, Temixco, Mexico

[d]Department of Geology, University of Pretoria, Pretoria, South Africa

* Corresponding author: Department of Geology,
University of Pretoria,
Pretoria 0002
South Africa
Tel.: ++27 (0)12 420 3310
Fax: ++27 (0)12 362 5219
E-Mail: nils.lenhardt@up.ac.za

Manuscript accepted by
Sedimentology

June 24, 2010

Build-up and depositional dynamics of an arc front volcaniclastic complex: the Miocene Tepoztlán Formation (Transmexican Volcanic Belt, Central Mexico)

ABSTRACT

Volcanic terrains such as magmatic arcs are thought to display the most complex surface environments on Earth. Ancient volcaniclastics are notoriously difficult to interpret as they describe the interplay between a single or several volcanoes and the environment. The early Miocene Tepoztlán Formation at the southern edge of the Transmexican Volcanic Belt (TMVB) belongs to the few remnants of this ancestral magmatic arc, and therefore is thought to represent an example of the initial phase of evolution of the TMVB. Based on geological mapping, detailed logging of lithostratigraphic sections, paleocurrent data of sedimentary features and AMS, mapping of 2D-panels from outcrop to field scale, and geochronological data in an area of c. 1000 km^2, three periods in the evolution of the Tepoztlán Formation were distinguished, which lasted around 4 million years and are representative of a volcanic cycle (edifice growth phases followed by collapse) in a magmatic arc setting. The volcaniclastic sediments accumulated in proximal to medial distances on partly coalescing aprons, similar to volcanic ring plains, around at least three different stratovolcanoes. These volcanoes resulted from various eruptions separated by repose periods. During the first phase of the evolution of the Tepoztlán Formation (22.8 – 22.2 Ma), deposition was dominated by fluvial sediments in a braided river setting. Pyroclastic material from small, andesitic-dacitic composite volcanoes in the near vicinity was mostly eroded and reworked by fluvial processes, resulting in sediments ranging from cross-bedded sand to an aggradational series of river gravels. The second phase (22.2 – 21.3 Ma) was characterized by periods of strong volcanic activity, resulting in voluminous accumulations of lava and tuff, which temporarily overloaded and buried the original fluvial system with its detritus. Continuous build-up of at least three major volcanic centers further accentuated the topography, and in the third phase (21.3 – 18.8 Ma) mass flow processes, represented by

an increase of debris-flow deposits, became dominant, marking a period of edifice destruction and flank failures.

Keywords: volcaniclastic, lithofacies analysis, facies model, Miocene, Transmexican Volcanic Belt

INTRODUCTION

The volcanic history of a magmatic arc is commonly best preserved in its associated sedimentary sequences, yielding essential information on depositional processes and often even the long-term evolution of volcanism (Smith & Landis, 1995; Orton, 1996; Einsele, 2000). Volcaniclastic deposits and their reworked sediments within a magmatic arc are inferred to represent the remains of ancient volcanic structures, i.e. stratovolcanoes (their aprons and distal basin fills), lava domes, intermediate and rhyolitic calderas, and monogenetic volcanoes. However, due to weathering, erosion and reworking with time, volcaniclastic successions commonly provide the only record of initial arc volcanism (Kuenzi et al., 1979; Vessell & Davies, 1981; Mathisen & Vondra, 1983; Ballance, 1988), particularly with respect to stratovolcanoes that are prone to erosion and can completely disappear within a few million years (e.g. Fisher & Schmincke, 1984; Riggs & Busby-Spera, 1991; Orton, 1996). The sedimentation, as well as the erosion and re-deposition of the sediments vary according to the contemporary climate and tectonic setting as well as the sediment supply (Geißler et al., 2008; Zernack et al., 2009). Stratovolcanoes, predominantly of andesitic-dacitic composition, are complex accumulations of lava flows, hypabyssal intrusive rocks and various types of tephra (e.g. Williams & McBirney, 1979). They build up over periods of tens or hundreds of thousands of years by repeated, relatively small-scale eruptions and are typical of convergent plate margins with thick continental crust (Cas & Wright, 1987; Palmer & Neall, 1991; Smith, 1991; Cronin et al., 1996; Orton, 1996; Davidson & De Silva, 2000; Donoghue & Neall, 2001; Borgia & van Wyk de Vries, 2003; Manville et al., 2009). During growth they constantly shed debris into the surrounding environment. This debris is provided either directly by means of aerial fallout from eruption columns, pyroclastic

flows, debris flows or by rivers, wind and glacial processes during inter-eruption periods. The sedimentary sequences associated with active volcanoes can be characterized by syn-, post- and inter-eruptive deposits resulting from the immediate or subsequent reworking of primary material by surface processes such as weathering and erosion. Smith (1991) sub-divided volcaniclastic sequences into syn-eruptive and inter-eruptive units, stating that syn-eruptive sequences result from primary volcanic processes and immediate reworking of volcaniclastic material. Manville (2002), however, redefined the syn-eruptive period as being limited by the last recognised phase of a single eruption and introduced the term post-eruptive period, comprising the period of landscape response to volcanic eruptions. Inter-eruption periods describe times where normal background sedimentary processes occur without a direct volcanic influence (Smith, 1991) and, which are mainly characterized by reworking and erosion of eruption-related deposits (Vessel & Davies, 1981; Scott, 1985; Smith, 1987).

Primary volcaniclastic rocks comprise the entire range of fragmental products deposited directly by explosive or effusive eruption, regardless of whether their transport occurs through air, water, granular debris, or a combination thereof (McPhie et al., 1993; White & Houghton, 2006). This includes all sediments or rocks of *pyroclastic*, *autoclastic*, *hyaloclastic* or *peperitic* origin (White & Houghton, 2006). All reworked units are considered as secondary volcaniclastic sediments. However, there is still a substantial grey area surrounding deposits of syn-eruptive processes such as eruption-triggered lahars and debris avalanches (Pierson, 1997; Capra et al., 2002), if they are to be considered as primary or secondary volcaniclastic rocks. The term epiclastic sediments may be restricted to fragments derived by weathering and erosion of pre-existing rocks, and excludes reworking of particles from non-welded or unconsolidated materials (e.g. Cas & Wright, 1987; Manville et al., 2009). Following Fisher (1961), these deposits are formed following weathering of volcanic (including volcaniclastic) rocks to produce new particles different in size and shape from the original volcaniclastic particles. Epiclastic sediments thus receive a sedimentary name with a volcanic modifier, such as tuffaceous sandstone or andesitic sandstone.

Accumulation is thickest near the volcanic cone and fine and deposits thin distally, giving rise to proximal-distal facies patterns (Vessell & Davies, 1981; Smith, 1988, 1991).

Subaerial radial ring-plains develop around isolated volcanoes (Palmer, 1991; Palmer & Neall, 1991; Palmer et al., 1993). The ring-plain system is a volcaniclastic apron that consists mostly of resedimented volcanoclastics as debris-flow, debris-avalanche and occasionally fluvial deposits that form related lithostratigraphic units (e.g. Cronin & Neall, 1997). Near shorelines, ring-plain systems can reach far into the sea (Karátson & Nemeth, 2001; Schneider et al., 2001), where pyroclastic flows and debris flows are transformed into subaqueous volcaniclastic debris flows and turbidity currents (Whitham, 1989; Cole & DeCelles, 1991). Ring-plain accumulation occurs during both constructional and destructional phases (e.g. Cas & Wright, 1987; Cronin & Neall, 1997). However, more commonly, linear aprons of volcaniclastic sediment develop adjacent to the volcanic arc (Mathisen & Vondra, 1983; White & Busby-Spera, 1987; Palmer & Walton, 1990; Runkel, 1990). The composition and facies associations of these volcanic aprons or ring plains are governed by the interplay between volcano-tectonic activity, different transport and depositional processes (Carey, 2000), and the climate, influencing weathering and transportation processes, giving insights into the interaction between an evolving volcaniclastic complex and its related material with existing drainage systems.

For this study, an up to 800 m thick, Early Miocene volcaniclastic sequence in an arc setting in Central Mexico was studied, using a wide set of different methods, including sedimentology, paleomagnetics, geochemistry, radiometric dating, and palynology to develop an evolutionary model. This volcaniclastic succession, called the Tepoztlán Formation (Fries, 1960), is one of the few remnants of the initial stage of the Transmexican Volcanic Belt (TMVB), forming spectacular cliffs south of Mexico City, that dominate the landscape around the villages of Malinalco, Tepoztlán and Tlayacapán in the States of México and Morelos. This formation is of particular interest because of: (i) ongoing discussion on the origin of the TMVB (Mooser, 1972; Demant, 1978; Cantagrel and Robin, 1979; Negendank et al., 1985; Nixon et al., 1987; López-Infanzón, 1991; Márquez et al., 1999; Verma, 1999, 2000, 2002; Sheth et al., 2000; Gómez-Tuena et al., 2003, 2007; Ferrari et al., 2005; Orozco-Esquivel et al., 2007); and (ii) because of its excellent outcrops, which allow study of the complex interaction of depositional processes at various scales, from thin sections to landscape panels.

In this paper, we focus on point (ii) and present a lithofacies analysis of sedimentological logs of type sections, and of outcrop photomosaics at various scales to unravel depositional processes and their control within time.

GEOLOGICAL SETTING

The TMVB is a continental magmatic arc, which comprises nearly 8000 volcanic structures (e.g. Gómez-Tuena et al., 2007). It is related to the subduction of the Cocos and Rivera plates under the North American plate along the Central American Trench, which was established during the Middle-Late Miocene (Ferrari et al., 2000). The TMVB is about 1000 km long and ranges from 80 to 230 km in width. In contrast to other subduction-related volcanic belts, running parallel to a deep-sea trench, the TMVB is obliquely orientated with respect to the Middle America Trench, forming an angle of about 16° (Gómez-Tuena et al., 2007). The belt consists of a large number of Tertiary and Quaternary cinder cones, maars, domes, and stratovolcanoes with predominantly calc-alkaline chemical and mineralogical compositions (Siebe & Macías, 2004). Recent studies have shown that the TMVB, as a distinctive geologic province, dates back to the Middle to Late Miocene, as a result of a counterclockwise rotation of the magmatic arc of the Sierra Madre Occidental (SMO; Ferrari et al., 1999). Little is known about the initial activity of the early arc because the main focus of previous studies was on younger volcanism (Márquez el al., 1999; Siebe et al., 2004; García-Palomo et al., 2002; Verma, 2000; Riggs & Carrasco-Núnez, 2004). The remnants of the ancestral TMVB are found close to the present volcanic front of the central sector of the arc as stated by several authors, such as in the Sierra de Mil Cumbres and Sierra de Angangueo volcanic complexes in the State of Michoacán (Pasquaré et al., 1991; Capra et al., 1997) and in the Malinalco area (State of México), where lavas were dated at 19.5 Ma (Ferrari et al., 2003) and 21 Ma (García-Palomo et al., 2000)); furthermore, in the deepest part of the Mexico City Basin (Ferrari et al., 2003). These rocks are considered to be part of the initial Early Miocene activity of the Transmexican Volcanic Belt (Gómez-Tuena et al., 2007). In later time, volcanism migrated further away from the trench, forming stratovolcanoes and lava cones, ranging in age from 15 to 10 Ma (Gómez-Tuena et al., 2007). These volcanic rocks can be found along the border of the states of Querétaro and Guanajuato (Carrasco-Núnez et al., 1989; Pérez-Venzor et al., 1996; Valdéz-Moreno et al., 1998; Verma & Carrasco-Núnez, 2003) and in the state of Puebla (Carrasco-Núnez et al., 1997; Gómez-Tuena & Carrasco-Núnez, 2000).

Another evidence of early volcanic activity of the TMVB is the Tepoztlán Formation, which has been neglected in studies on the initial phase of the Transmexican Volcanic Belt so far.

The study area (18°54'-19°01'N lat., 98°57'-99°32'W long.) covers approximately 1000 km^2 and is located along the southern edge of the TMVB (Fig. 1), where the Tertiary volcaniclastic series of the Tepoztlán Formation are covered by Quaternary lavas and scoria of monogenetic volcanoes of the Chichinautzin volcanic field. Within this area, the Tepoztlán Formation crops out in an area of 180 km^2 and has an overall maximum thickness of 800 m. The volume of the deposited material remaining after erosion was calculated at 130 km^3 with the help of a geographic information system (GIS). The formation is widespread around the villages of Malinalco and Chalma in Mexico State and Tepoztlán and Tlayacapan in Morelos State; sparse outcrops are located east of Tlayacapan and southeast of Nevado de Toluca (Capra & Macías, 2000; García-Palomo et al., 2002).

A variety of Eocene-Oligocene (Balsas Group) and older rocks, mostly Cretaceous limestones, underlie the formation. It is covered by lava flows of Pliocene to Holocene age. Close to Malinalco the Tepoztlán Formation crops out between the San Nicolás Basaltic Andesite and the overlying Basal Mafic Sequence (García-Palomo et al., 2000). The formation of the San Nicolás Basaltic Andesite at 21.6 ± 1.0 Ma (García-Palomo, 1998) suggests deposition contemporaneous with the Tepoztlán Formation (Lenhardt et al., 2010). However, closer field relationships between both formations have not been studied yet. In Tepoztlán and the eastern vicinities the Tepoztlán Formation unconformably overlies the Balsas Group and is covered by the Chichinautzin Formation.

The Tepoztlán Formation has traditionally been described as consisting of massive lahars rich in subrounded porphyritic andesite clasts intercalated with fluvial deposits (Fries, 1960; De Cserna & Fries, 1981a). The formation is composed of calc-alkaline volcanic and sedimentary rocks. The volcanic rocks have predominantly andesitic to dacitic compositions; however, rhyolites are also present (Lenhardt, 2009). The entire succession comprises pyroclastic deposits (fall, surge and flow deposits), deposits from lahars (debris-flow and hyperconcentrated-flow deposits), and coarse to fine fluvial and

lacustrine deposits (conglomerates, sandstones and mudstones). Only few lava flows and dikes are present.

Bedding within the Tepoztlán Formation is generally flat-lying or gently dipping at up to 10° to the N/ NNE. The succession is disrupted by normal faults and sub-volcanic intrusions. Fault displacements are frequently about half a meter and rarely exceed a few meters.

Magnetostratigraphy combined with K/Ar and Ar/Ar geochronology revealed an Early Miocene age (22.75-18.78 Ma, Fig. 2). The formation can further be subdivided into three units, according to the dominant mode of deposition: (1) the lower fluvial-dominated Malinalco Member (22.8 – 22.2 Ma); (2) the middle eruptive-dominated San Andrés Member (22.2 – 21.3 Ma); and (3) the upper debris-flow-dominated Tepozteco Member (21.3 – 18.8 Ma; Lenhardt et al., 2010).

Within the study area, the Lower Miocene (Upper Aquitanian – Lower Burdigalian) was characterized by a period of cool temperate and humid climate, pointing to an already highly elevated area that was probably strongly affected by the monsoon (Lenhardt, 2009).

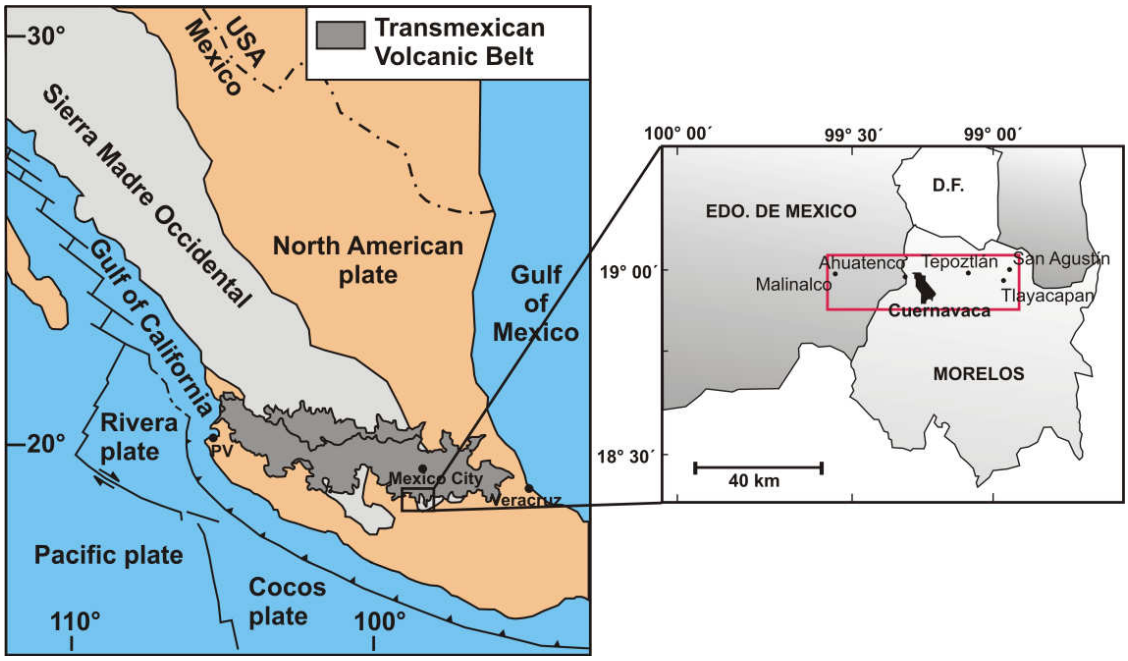

Figure 1. The extension of the TMVB in Central Mexico and the location of the study area.

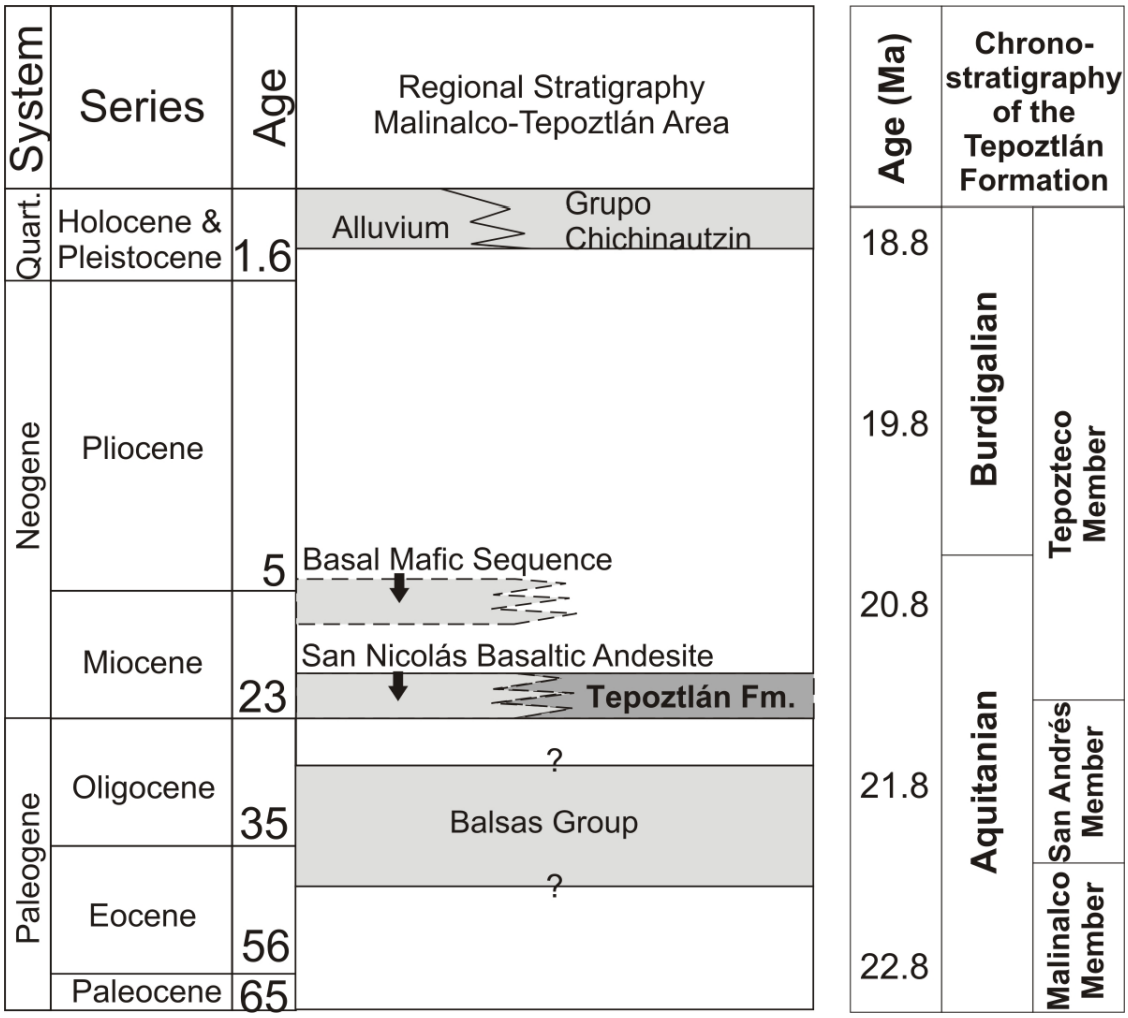

Figure 2. Simplified stratigraphic column of the study area (after García-Palomo et al., 2000 and Lenhardt et al., 2010)

METHODS AND DATABASE

This study is based on an integrated analysis of lithological and sedimentological data from the Tepoztlán Formation. Ten stratigraphic columns, ranging in thickness from 25 to 448 m, were measured and recorded, spanning 56 km along strike, representing the range of sedimentary environments characteristic of the Tepoztlán Formation (Fig. 3-4). In addition, 22 2D-outcrop panels were obtained to study the complex interaction of fluvial, eruptive and gravitational processes at three different scales and combined into a

lithofacies model. At small-scale, optically corrected photomosaics (Wizevich, 1991; Arnot et al., 1997) were obtained from the outcrop walls to be able to determine the size of different architectural elements. At first, the outcrop wall is marked with regularly and perpendicular to the wall placed stadia rods as scales. Afterwards, the picture frame is determined. Pictures of the outcrop wall were taken by means of several overlapping photographs. The overlapping has to be at least 25% on each side to avoid optical distortion. For photography, the camera has to be positioned on a line at right angles from the picture center at the outcrop wall. By giving the camera the same inclination as the outcrop wall (picture plane parallel to wall plane) optical distortion is avoided. The digital pictures are finally put together and distorted in a panorama program. The architectural elements and major sedimentary structures were then mapped from the corrected photomosaics.

For medium-scale (steep side of a hill or mountain) or large-scale (mountain range) this precision was not possible and photomosaics were created from a further distance without scales. However, to improve the exactness of the wall panels and to collect detailed information about the grain size, sedimentary structures and lithologic parameters, a vertical profiling along selected sections was carried out.

Vertical and lateral distribution of depositional units together with stratigraphical data (K/Ar and Ar/Ar geochronology combined with paleomagnetic studies; Lenhardt et al., 2010) were used to reconstruct the temporal evolution of the depositional environment and to identify volcanic centers. In addition, more than 200 paleocurrent indicators (Anisotropy of Magnetic Susceptibility and sedimentary structures) were measured to constrain dispersal patterns and locate source areas. Along with sedimentological paleocurrent analysis, mostly based on clast imbrication, channel-wall orientations and cross-stratification (from three-dimensional exposure), the paleomagnetic Anisotropy of Magnetic Susceptibility (AMS) technique (see Lenhardt (2009) for methodology) has been used successfully. AMS is a relatively fast and inexpensive method that yields three-dimensional flow markers (Cañón-Tapia & Castro, 2004). The susceptibility depends on the rock's minerals and their relative amounts, and, in the case of primary volcanic rocks, is mainly related to the magma chemistry and crystallization conditions (Zanella et al., 1999). These crystals also determine the susceptibility in the resulting

deposits after erosion and redeposition, i.e. the epiclastic fluvial and mass-flow deposits (Lenhardt, 2009). Application and results of this method will be addressed in more detail in a separate paper. However, the results of these studies are used here to locate the provenance of fluvial deposits as well as the source vent locations of volcanic products.

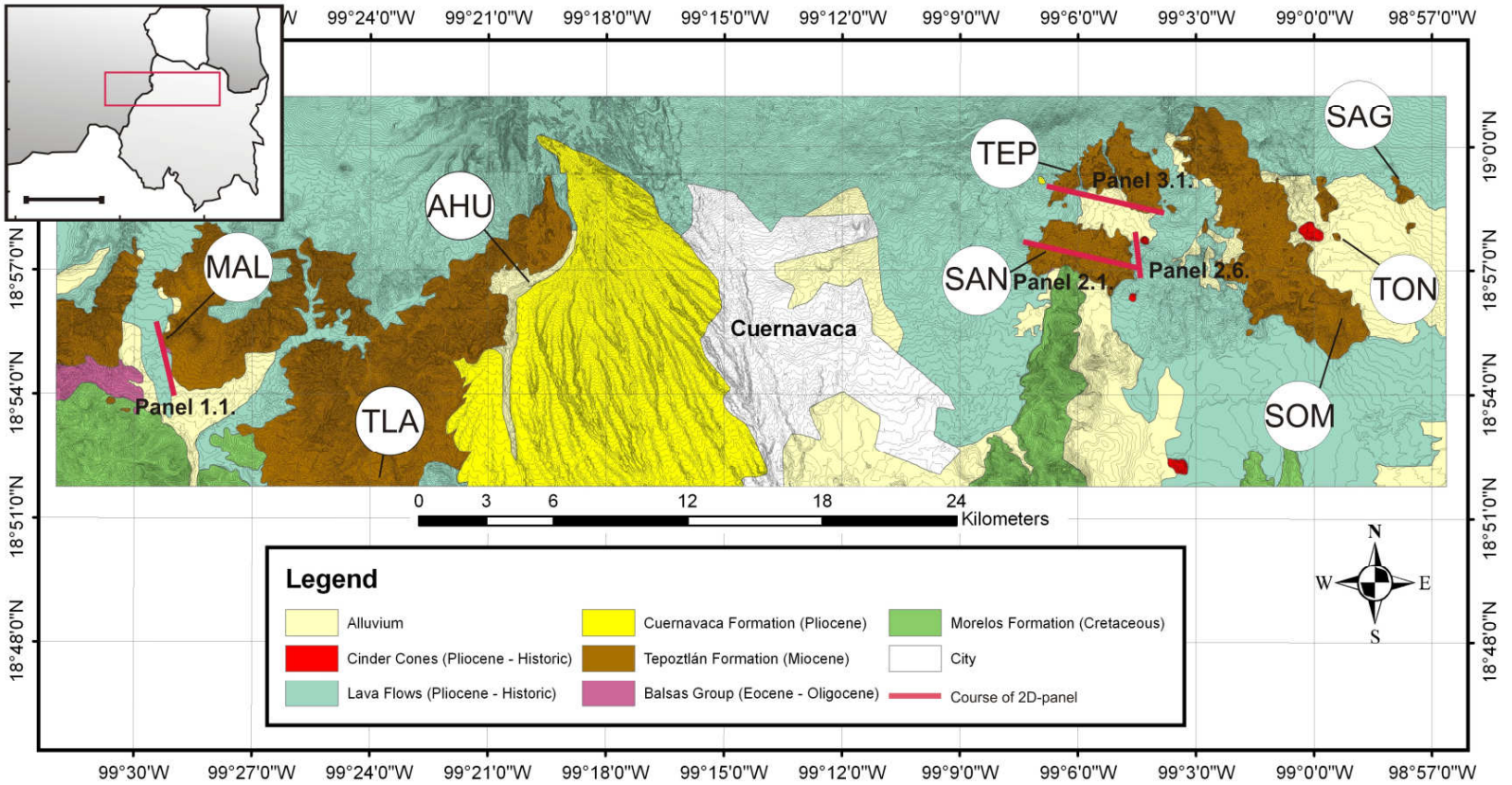

Figure 3. Geological map of the study area with the locations of sampled sections and large-scale 2D-panels. The locations of stratigraphic sections are shown by red lines. Outcrop locations are: MAL – Malinalco; AHU – Ahuatenco; TLA – Tlajotlán; TEP – Tepozteco; SAN – San Andrés; SOM – Cerro Sombrerito; TON – Cerro Tonantzin; SAG – San Agustín.

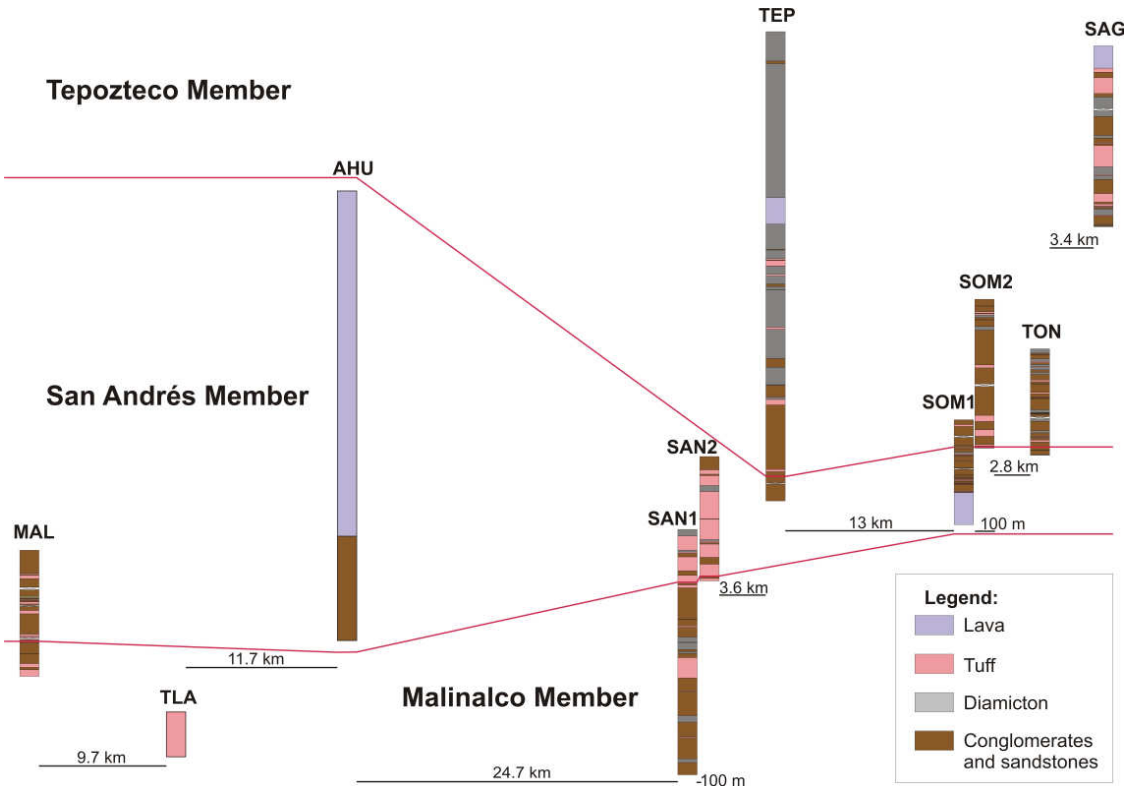

Figure 4. Stratigraphy of the Tepoztlán Formation conducted over 56 km along strike, showing correlations between outcrops. The locations of the sections are indicated in Fig. 3.

VOLCANO-SEDIMENTARY LITHOFACIES

The Tepoztlán Formation comprises 12 volcanic and sedimentary lithofacies distinguished on the basis of rock type, sedimentary and volcanic structures or textures, and grain size (Table 1). The subdivision into syn-eruptive, post-eruptive and inter-eruptive deposits is derived from Smith (1991) and Manville (2002), and is further subdivided into primary volcanic and volcaniclastic, secondary volcaniclastic and epiclastic accumulations.

Table 1: Compilation of the lithofacies types, their interpretation and depositional processes.

Lithofacies	Interpretation		Processes	
Andesitic-dacitic volcanic lithofacies	LF	Lava	syn-eruptive	primary volcanic
Massive, parallel bedded lapilli lithofacies	FA	Pyroclastic fall deposit		
Stratified and cross-stratified tuff lithofacies	SU	Pyroclastic surge deposit		
Massive lapilli-tuff lithofacies	AF	Ash-flow deposit		
Massive tuff breccia lithofacies	BA	Block-and-ash flow deposit		
Pumiceous diamicton lithofacies	DF	Debris-flow deposit	post-eruptive	secondary volcanic
Pumiceous diamicton with diffuse cross-stratification lithofacies	HF	Hyperconcentrated-flow deposit		
Cross-bedded tuffaceous conglomerate lithofacies	GB	Gravel bar	inter-eruptive	fluvial
Cross-stratified tuffaceous sandstone lithofacies	CH	Channel-fill		
Erosional scour with intraclast lithofacies	SC	Scour pool-fill		
Planar-bedded to low-angle cross-bedded tuffaceous sandstone lithofacies	SF	Sheet flood deposit		
Tuffaceous silt- and claystone lithofacies	LC	Lacustrine deposit		lacustrine

Syn-eruptive deposits

Primary volcanic/ volcaniclastic deposits

LF 1: Andesitic-dacitic volcanic lithofacies

The 15-25 m-thick flows within the Tepoztlán Formation commonly have a blocky carapace and a dense core, being exposed either on the top of mountain ridges or intercalated between other depositional units, and exhibit an irregular, unconformable contact to the underlying deposits. Angular fragments of the carapace range from 3-50 cm in size at the base or the top of massive flows. The dense core can show columnar jointing. All flows have a porphyritic to glomeroporphyritic texture. Plagioclase is the most abundant phase with subordinate K-feldspar, clinopyroxene and amphibole. Accessory phases consist of mica, abundant titanomagnetite and other accessories

(Lenhardt et al., 2010). The groundmass shows a hyalophylitic, sometimes trachytic texture, comprised of plagioclase microlites and an ore phase (titanomagnetite). The whole rock SiO_2 content of the lavas ranges from 55.9 to 60.6 wt.%, identifying them as andesites or dacites (Lenhardt, 2009).

The volcanic facies, represented by andesites and dacites are interpreted as viscous, slow moving blocky lava flows (LF) (MacDonald, 1972; Mueller, 1991) as they are associated with lava domes and coulées, rarely exceeding 1-2 km in flow length (Williams & McBirney, 1979; Orton, 1996). The massive to brecciated units display the attributes of a coherent flow in which autobrecciation processes were prevalent and produced breccia during flow advance (Bonnichsen & Kauffmann, 1987).

Tuff facies

Within the study area abundant tuff layers are exposed. Each unit consists of a massive to finely laminated or cross-bedded, varicolored, poorly sorted mixture of medium to coarse ash horizons, sometimes rich in lapilli. Unit thicknesses range from a few centimeters to several meters. Based on texture and lithology four subfacies were distinguished, tentatively attributed to pyroclastic fall deposits (one subfacies) and pyroclastic density current deposits (three subfacies). Pyroclastic density currents are hot gas-particle dispersions whose density generally exceeds that of the atmosphere or hydrosphere into which they are introduced (Branney & Kokelaar, 2002).

LF 2: Massive, parallel bedded lapilli-tuff lithofacies

This facies is characterized by massive or crudely plane-bedded tuffs, with uniform thicknesses between 5 and 10 cm that drape underlying irregularities and can be traced for several hundred meters throughout the outcrops. The layers consist of coarse ash and lapilli particles, showing either normal or inverse grading. Constituent grains are very angular and are composed of pumice particles and pyroxene crystals of the same grain size.

This facies is interpreted as a pyroclastic fall deposit (FA). Reverse and normal grading can be attributed to a change in the dynamics of the eruption system (e.g. column height, vent radius, vent flaring; Carey & Sigurdsson, 1989), suggesting waning or waxing

eruption intensities. The localized preservation of pyroclastic fall deposits within the study area depended on the rapid accumulation of protective cover, either as reworked or additional primary volcaniclastic material.

LF 3: Stratified and cross-stratified tuff lithofacies

The stratified tuff forms thin (5-10 cm in thickness) discontinuous layers, is moderately sorted, mostly composed of a coarse ash matrix with pumice fragments of ash to lapilli size. Pumice lapilli show signs of abrasion. The dominating grading pattern is fining-upward, suggesting waning flow energies. The stratification varies from subparallel, through pinch-and-swell stratification to cross-stratified tuff. The lower surfaces can be flat, although local erosional surfaces can be recognized.

The deposits are interpreted as being deposited under surge-like depositional conditions from dilute gravity currents or during windy conditions (Allen et al., 1999) and are interpreted as pyroclastic surge deposits (SU). The subparallel stratification, cross-stratification, and moderate sorting indicate deposition from traction-dominated flow boundaries (Branney & Kokelaar, 2002). The subparallel stratification differs from ash-fall lamination in that individual laminae are discontinuous and the lithofacies exhibit grain fabrics (Cagnoli & Tarling, 1997). Pyroclastic surge deposits usually attain a small volume (< 1 km^3) and rarely reach more than 10 km from their source (Orton, 1996).

LF 4: Massive lapilli-tuff lithofacies

The massive pumice-rich tuffs exhibit a wide range of grain-sizes, covering everything from fine ash to cobble-sized lithic and pumice clasts (max. 10 cm) and mainly consist of accessory and minor accidental lithic fragments in a matrix of bubble wall shards and phenocrysts (feldspars, augite, rare quartz). They are generally non-welded, however, moderate welding without signs of vapour-phase crystallization was recognized locally. Accessory lithic clasts are comprised of gray to red porphyritic rocks of dacitic to andesitic composition (58.5 - 66.5 vol.% SiO_2; Lenhardt, 2009). Pumice clasts range from creamy white to pale yellow in color. They are relatively dense to finely vesicular and usually porphyritic, containing predominantly augite and plagioclase as phenocrysts. Within the matrix, pumice clasts usually do not exceed diameters of 6 mm. However, in

pumice concentration zones on top of single units, clasts can reach up to 10 cm in diameter. Due to transportation and abrasion they appear subrounded to rounded. The deposits usually show a normal coarse-tail grading of the lithic clasts while the pumice clasts show a reverse grading. Thicknesses of single units can vary from 0.1 to 9.0 m with an average of 1.5 m. The deposits partly drape the pre-eruption topography, thickening in valleys and depressions. Their lower bounding surfaces are flat or reflect the paleosurface, their tops are mostly eroded. The deposits occur as single units or as a series of stacked beds.

The massive lapilli-tuff lithofacies is interpreted as ash-flow deposit (AF) and is described by many authors as the most common ignimbrite lithofacies (e.g. Ross & Smith, 1961; Sparks, 1976; Wilson & Walker, 1982; Branney & Kokelaar, 2002). Very large ash flows, from Plinian eruptions of dacitic to rhyolitic magma, are reported to have traveled over 100 km from their source (Orton, 1996). However, smaller volumes and traveled distances are reported from andesitic to basaltic ash flows (e.g. Robin et al., 1994; Freundt & Schmincke, 1995).

LF 5: Massive tuff breccia lithofacies

This lithofacies is characterized by massive, matrix-supported, poorly sorted monolithological tuff breccias. Thicknesses vary from 1.1 to 2.7 m with an average of 1.8 m. The deposits pinch out laterally and exhibit flat or erosive bases and flat upper surfaces. Grading patterns are absent. The tuff breccia consists of angular, oxidized, nonvesiculated dacitic to andesitic clasts in a fine-grained ash and lapilli matrix of the same chemical composition, pointing to a co-genetic origin. Pumice clasts as well as welding features are absent. Many lithic blocks exceeding 0.5 m in diameter exhibit radial prismatic fractures, breadcrust structures or expansion cracks indicative of *in situ* cooling from high temperatures (Lock, 1978; Carrasco-Núnez, 1999). The matrix is made up of glass shards, lava fragments and abundant phenocrysts resembling the crystal content of the clasts.

The massive tuff breccia lithofacies is interpreted to be derived from block-and-ash flows. Block-and-ash flow deposits (BA) result from small-volume pyroclastic flows, generated by explosive disruption or the sudden gravitational collapse of silicic lava

flows or domes (Wright et al., 1980; Francis, 1994; Freundt et al., 2000). Block-and-ash flows from gravitational collapse or weak explosions usually produce thick, valley confined, high-concentration, high-yield strength flows with well-defined deposit fronts and margins (Orton, 1996). This lithofacies is mostly confined to proximal to medial exposures. Block-and-ash flows, resulting from small-scale eruptions from Mt. Taranaki in New Zealand were confined to within 15 km of their parent summit dome (Platz et al., 2007), BA's from Soufriere Hills went about 7 km away from their source (Calder et al., 2002). The coarse grain-sizes and the lack of associated lava flows of this lithofacies within the study area suggests proximal to medial deposition less than 10 km away from the source (c.f. Valentine, 1987).

Post-eruptive deposits

Secondary volcaniclastic deposits

LF 6: Pumiceous diamicton lithofacies

This lithofacies is composed of angular to subangular clasts in a pinkish red matrix of fine to medium sand. They occur in laterally extensive (up to several 100 meters) sheets with planar bases and eroded tops. Average thicknesses of single units are about 4 m; however, vertical amalgamation surfaces between stacked units are rarely visible, resulting in deposits up to 14 m thick without any visible bounding surfaces. The deposits show no signs of grading or sorting. The clast size usually is in the range of pebbles and cobbles, not exceeding diameters of 20 cm; however, single outsized clasts of 2 m in diameter have been observed especially near Santo Domingo (19.00°N, 99.03°W). The clast characteristics and compositions within these deposits are similar to that of the massive tuff breccia (LF 5), suggesting that this lithofacies represents remobilized pyroclastic flows (c.f. Siebe et al., 1993; Carrasco-Núnez, 1999). The prevalence of angular to subangular intermediate volcanic clasts implies a local source, and thus contemporaneous volcanism and sedimentation. The matrix of the deposits is commonly composed of lithic and pumice fragments, crystals and glass shards, showing significant alteration to clay minerals. The fragments do not show any alignment within the matrix.

The poor sorting and massive appearance are evidence for transport and deposition of this lithofacies by and from debris flows (DF) (Hampton, 1975; Johnson & Rodine, 1984; Smith & Lowe, 1991; Coussot & Meunier, 1996; Pierson et al., 1996). The occurrence of prismatically fractured clasts in debris-flow deposits suggests that the debris flows were generated by mixing of water with recently emplaced debris from block-and-ash flows (e.g. Smith, 1986, 1988).

LF 7: Pumiceous diamicton with diffuse cross-stratification lithofacies

This lithofacies is similar to the previous one, in extent as well as in the appearance of their bounding surfaces, showing lateral extensive sheets up to several 100 m wide and often planar surfaces. This lithofacies, however, shows a weakly defined and widely spaced low-angle cross-stratification, normal or inverse grading and locally scoured lower contacts. Thicknesses vary between 0.1 and 6 m within the study area.

This lithofacies is interpreted on the basis of the faint stratification to have been deposited from hyperconcentrated flows (HF) rather than debris flows (Pierson & Scott, 1985; Coussot & Meunier, 1996; Sohn et al., 1999). The term hyperconcentrated flows (Beverage & Culbertson, 1964; Smith, 1986) is used to describe deposits from flows with sediment concentration intermediate between debris flows and fluvial floods.

The lithofacies representing deposition by debris flow and hyperconcentrated flow, best characterize lahar processes that acted across the Tepoztlán Formation aprons (e.g. Walton & Palmer, 1988). The term lahar describes all rapidly flowing mixtures of rock debris and water (other than normal streamflow) from a volcano (Smith & Lowe, 1991). Lahars can either be syn- or post-eruptive (Vallance, 2000), be a direct result of eruptive activity or happen up to decades after an initial eruption, a link that is difficult or impossible to establish in ancient successions (Orton, 1996). However, no hydrothermal alteration, no cooling cracks, and no carbonized plant fragments were found within the deposits, which is why no direct result of eruptive activity is assumed. Paleovegetation patterns confirm humid continental climatic conditions in the study area during accumulation of the Tepoztlán Formation (Lenhardt et al., 2008) with dry winters, monsoonal type rainfall during the summer and rainfall intensities of 20-220 mm/month throughout the year (Lenhardt, 2009). Furthermore, the paleovegetation points to an

already highly elevated area. Given the paleometeorologic setting and probable slope characteristics of the volcano, the intense rainfall and the resulting runoff on the volcano's slopes probably triggered rain-lahars as described by Rodolfo & Arguden (1991). Lahars usually travel 10's to 100's of km from their source (Einsele, 2000), e.g. a lahar from the 1877 eruption of Cotopaxi travelled 270 km (Orton, 1996).

Inter-eruptive deposits

Fluvial deposits

LF 8: Cross-bedded tuffaceous conglomerate lithofacies

This lithofacies is poorly sorted with a grain-size distribution from fine sand to cobbles. Gravel particles, representing the main grain-size are subangular to subrounded. The coarsest cobbles and boulders are usually up to 20 cm across. Locally, lenses of cross-stratified sandstone occur. The matrix dominantly consists of sand grains, resembling small clasts of lava, pumice or ash particles. The conglomerates form single beds or sets of stacked beds. Individual beds can be separated by thin sandy layers. Thicknesses vary from 0.2 to 6 m with an average of 1 m. The conglomerates show flat or concave lower bounding surfaces, pinching out laterally. Lenticular strata are bounded by scour surfaces. Laterally, extensions range from few meters up to several tens of meters. Preferred clast orientation occurs parallel to bedding in cross-stratified units.

This lithofacies is very common in gravel-bedload stream deposits (e.g. Steel & Thompson, 1983; Smith, 1990; Siegenthaler & Huggenberger, 1993) as they appear in sheets and lenses as manifested in gravel bars (GB) in braided river systems (e.g. Miall, 1977). The movement of sediment in gravel-bed rivers commonly occurs in pulses (Whiting et al., 1988; Reid & Frostick, 1987). A close relationship between movement of sand and initiation of entrainment of gravel is described resulting in a wavelike transport process (Kuhnle, 1996).

LF 9: Cross-stratified tuffaceous sandstone lithofacies

This lithofacies consists of gray tuffaceous sandstones, comprising glassy material, small lava and pumice particles and minor rounded phenocrysts, dominated by feldspars and pyroxenes. Trough cross-bedding is the dominant sedimentary structure. However, planar cross-bedding or scour-fill bedding is also common. Individual units are stacked, often forming multilateral and single- or multistorey packages. The thicknesses of the units range from 0.1 to 6 m with an average of 0.8 m. The lateral extent cannot be determined clearly in all cases; however, some outcrops show extents of up to 150 m. They are characterized by erosive, concave-up to flat bases. Laterally, individual elements pinch out or are completely eroded away. Subangular to subrounded, pebble- to cobble-sized clasts (up to 20 cm) are concentrated on erosional contacts. Fining-upward successions are common, often with clayey ripple cross-laminated layers on top.

Based on the composition, the presence of crystals and the absence of basement material, the original fragmentation process and components support an initial pyroclastic origin. However, the sedimentary structures indicate significant reworking of either primary pyroclastic material or material that had already previously been reworked by lahars. Cross-stratification with unimodal paleocurrent pattern, fining-upward sequences, and channel scours at the base are all consistent with fluvial channel fill (CH) (Miall, 1978; Walker & Cant, 1984). Trough cross-stratification indicates infilling of a channel by bedload in the form of migrating bedforms (Miall, 1977; Harms et al., 1982; Siegenthaler & Huggenberger, 1993; Kataoka, 2005). Planar-cross bedded sediments are typically interpreted as the deposits of migrating straight-crested dunes, generally formed within the deeper portion of the active channel (Miall, 1985), or by avalanching on the slipfaces of simple bars (Miall, 1996). Such bars may have either been bank-attached (lateral bars) or detached as transverse or medial bars (Todd, 1996). Thus, the deposits of this facies are interpreted as channel fill in a braided river. Fining-upward sequences resulted from the lateral migration of streams or a deceleration in flow velocity due to a decrease in channel activity. Multistoried fining-upward packages with erosional bases suggest frequent channel reactivation with development of bars in fluvial systems. Pebble- to cobble-sized clasts on erosional surfaces were deposited as a lag deposit on a channel floor. Clast abrasion in streams was rather inefficient as shown by the subangular to subrounded shapes, which is why it is supposed that all clasts were deposited at a

proximal to median distance from the source area. The fine, clayey layers on top of this lithofacies points to very low flow energies after relocation of the main channel.

LF 10: Erosional scour with intraclast lithofacies

This lithofacies is characterized by an erosive, concave-up lower bounding surface. If the upper surface is eroded, an interaction with other facies is observed. The internal structure consists of trough cross-bedded gravels and sand. Thicknesses can range from 0.1 to 6 m with an average of 0.8 m.

This lithofacies is interpreted to represent scour pool fills (SC) formed within channels as they are most common within braided rivers (Miall, 1977, 1978).

LF 11: Planar-bedded to low-angle cross-bedded tuffaceous sandstone lithofacies

This lithofacies, generally consisting of medium to coarse sand, is locally preserved within gravel deposits. It always occurs in multistoried sequences consisting of horizontal beds, ranging from 0.1 to 0.8 m thick with an average of 0.2 m. The beds show a generally sheet-like geometry, but locally bifurcate or pinch out laterally. Individual beds can extend more than 150 m before pinching out or being eroded laterally. Underlying beds can be locally scoured. The lithofacies can show normal grading, although an inverse grading is dominant.

Low-angle cross-bedding, in association with planar-bedded sediments, is common in fluvial sandstones (Segschneider et al., 2002). These lithofacies are interpreted as upper-stage plane bed deposits as they are typical for sheet-flood deposits (SF) (Blair, 1987; Blair & McPherson, 1994; Chamyal et al., 1997) and unconfined flash-flood deposits (Miall, 1985) on alluvial fans. Their preservation potential within a gravel-bed river is relatively low (Kostic et al., 2007) for which reason Palmer & Walton (1990) propose an emplacement in the distal part of an alluvial fan.

LF 12: Tuffaceous silt- and claystone lithofacies

Several thin strata of red to purple tuffaceous siltstones and claystones are recognized within the study area. They appear massive or laminated and rarely exceed thicknesses of more than one or two cm. However, at some locations such as near Malinalco, silt- and

claystones reach thicknesses of several meters. The sediments contain abundant pumice and ash particles. Transitions from inversely graded, clast-rich deposits to fine-grained (ungraded or normally graded), matrix-supported deposits occur.

The thin sheet- or lens-shaped deposits are interpreted as waning flood sediments. The purple color probably represents subaerial alteration (Jo et al., 1997). However, no real paleosoils could be found throughout the whole sequence. Near Malinalco and in the east of the village of Santo Domingo in the State of Morelos (19.00°N, 99.03°W), siltstones several meters thick, coarsening-upward, are interpreted as lacustrine deposits (LC). The coarsening-upward is interpreted as deposition near the lake-shore with steady accumulation of sediment in a progradational setting. Outsized pumice clasts, locally "floating" in matrix support in this lithofacies, are interpreted to have been formed by suspension settling within lakes or ponds (Collinson, 1996; Manville et al., 2002).

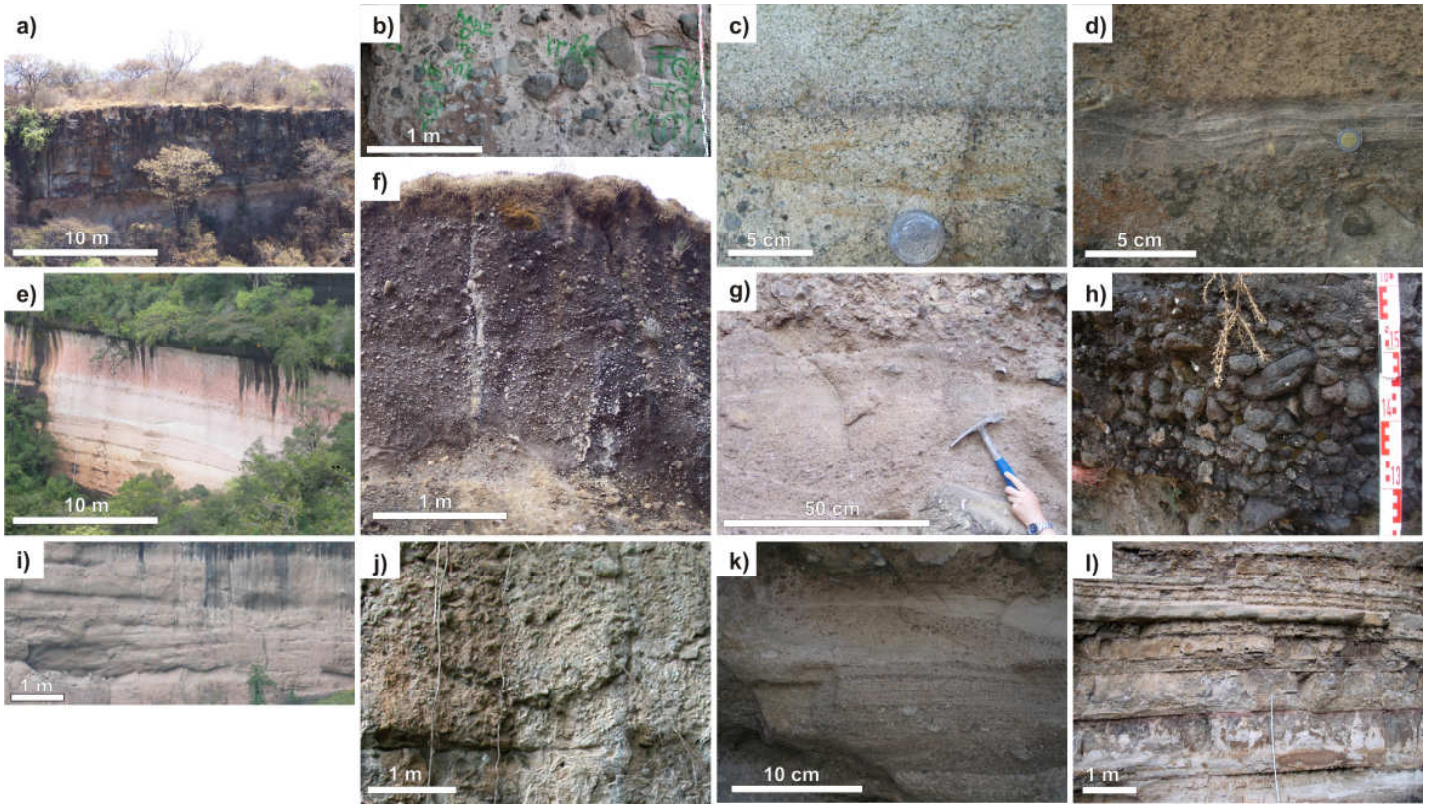

Figure 5. Photographs showing examples of the lithofacies types/ architectural elements: a) LF 1: LF (lava flow), b) LF 2: FA (pyroclastic fall deposit), c) LF 3: SU (pyroclastic surge deposit), d) LF 4: AF (ash-flow deposit), e) LF 5: BA (block-and-ash flow deposit), f) LF 6: DF (debris-flow deposit), g) LF 7: HF (hyperconcentrated-flow deposit), h) LF 8: GB (gravel bar), i) LF 9: CH (channel-fill), j) LF 10: SC (scour-fill), k) LF 11: SF (sheet-flood), l) LF 12: LC (lacustrine).

LITHOFACIES ASSOCIATIONS

The facies architecture of volcaniclastic aprons is typically complex, reflecting alternating periods of high-volume sedimentation in response to eruptive activity, and low-volume sedimentation in inter-eruption intervals (Vessel & Davies, 1981; Palmer & Neall, 1991). According to Smith & Landis (1995), the sedimentary and volcanic deposits associated with arc volcanism can generally be divided into three general facies associations, which can give information about proximal-distal relationships to a possible volcanic vent: central, apron, and distal facies:

Central facies association (0-10 km):

In general, proximal facies corresponding to a volcanic edifice comprise lava flows, autoclastic and pyroclastic breccias and intrusions (Smith & Landis, 1995). Debris-flow deposits are present but not abundant and some of the accumulations show hydrothermally altered debris (Palmer & Walton, 1990).

Apart from dacitic lava domes and coulées, only in one location direct evidence for a larger-scale volcanic structure could be identified within the Tepoztlán Formation. In Tlajotlán (18°52’ N, 99°23’ W; Fig. 3), a very coarse volcanic breccia interpreted as a vent breccia and intruded by various dikes spreads over an area of c. 6 km^2. The thickest lava flows within the study area can be found close to Ahuatenco where they reach thicknesses of up to 400 m, filling up a deep paleovalley and smoothing the landscape on top. Ahuatenco is situated c. 6 km away from the Zempoala complex whose eruptive history is known since at least the late Miocene (De Cserna & Fries, 1981b), and whose proto-edifice is supposed to be one source for the Tepoztlán Formation (De Cserna & Fries, 1981a). Furthermore, in San Andrés, at Cerro Tepozteco, Cerro El Sombrerito and San Agostín up to 25 m-thick lava domes or coulées could be identified. However, abundant dikes intruding the sequence in these locations gave younger dates (15.83 ± 1.31 Ma; Lenhardt et al., 2010) and can thus not be related to a possible main vent area.

Apron facies association (5-35 km):

Apron facies generally includes rapidly deposited volcanic and sedimentary materials that encircle individual volcanoes or form prism-shaped accumulations of debris flanking the arc and contributed from many vents (Smith & Landis, 1995). The sedimentary strata are composed mostly of event deposits related directly or indirectly to the stripping of loose volcaniclastic debris from steep volcanic slopes during or shortly following eruptive episodes (Vessel & Davies, 1981; Smith, 1987; Palmer & Walton, 1990). Primary volcanic components in the apron facies include rare (low-viscosity) lava flows, ignimbrites, and fine- to coarse-grained fallout tephra (Smith & Landis, 1995). The dominance of debris-flow and hyperconcentrated-flow facies in continental volcaniclastic aprons, or ring plains (Hackett & Houghton, 1989) results in deposition of sediment that may resemble non-volcanic alluvial fans. Fluvial sandstone fills the base of most channels; others are filled by debris-flow or hyperconcentrated-flow deposits only (c.f. Palmer & Walton, 1990). In connection with the apron facies association, Siebe et al. (1991, 1993) describe block-and-ash fans, composite accumulations of many pyroclastic flows, flood deposits, and debris flows that are channelled through valleys on the slope of the volcano toward its base where they deposit. Siebe et al. (1993) further describe these block-and-ash fans as principally consisting of a succession of breccia deposits with many unconformities, very similar in appearance to parts of the Tepoztlán Formation.

The apron facies association characterizes the major part of the Tepoztlán Formation, represented by the San Andrés and the Tepozteco Members in the locations Malinalco, San Andrés, Tepozteco, Sombrerito and San Agostín. Here, upper reaches are dominated by debris-flow and hyperconcentrated-flow deposits, up to 40 m-thick pyroclastic flow deposits, coarse-grained pyroclastic fall deposits and coarse fluvial conglomerates.

Distal facies association (20-70 km):

In general, the distal facies association represents terminal deposition at sites that receive little direct volcanic impact from eruptive events (Smith & Landis, 1995). In non-marine sedimentary basins, deposition of this facies association is mostly concentrated on fluvial system deposits and overbank alluvium (Smith, 1988; Hackett & Houghton, 1989; Riggs & Busby-Spera, 1990). Primary volcanic products are generally restricted to fine-grained fall deposits and far travelled ignimbrites comprising minor contributions to the

stratigraphy (Smith & Landis, 1995). The mostly non-volcanic sequences can include tuff layers deposited by atmospherically transported ash hundreds or thousands of km from the source volcano. Typical volcaniclastic beds of this distal facies association can comprise cm- to dm-thick primary pyroclastic fall deposits overlain by meter- to 10's of m-thick resedimented volcaniclastic deposits, intercalated in sedimentary successions of non-volcanic provenance (c.f., Kataoka et al., 2009).

The distal facies association characterizes the lower part of the Tepoztlán Formation, mostly represented by the Malinalco Member in Malinalco and San Andrés but also by the San Andrés Member at the Cerro Tonantzin. Here, deposition is dominated by sandstones and conglomerates, resulting from sheet floods and fluvial sediments in a braided river system. Only relatively thin pumiceous diamicts are present in these locations, resulting from hyperconcentrated flows. Ignimbrites and pyroclastic fall deposits are very rare and only appear in thin layers.

DEPOSITIONAL ARCHITECTURE

The eight analyzed locations display successions of volcanic, primary and secondary volcaniclastic, and fluvio-lacustrine deposits over areas several hundred meters in width and height. Of the eight analyzed locations, three key locations, which gave the names for the three stratigraphic members (Malinalco, San Andrés and the Tepozteco) are described in detail. For more elaborate descriptions of the remaining sections read Lenhardt (2009). Lithostratigraphic sections are discussed in context with related medium-scale panels. Where appropriate, descriptions of small-scale panels are included to verify interpretations by analyzing the spatial distribution of different lithofacies with a detail that can not be described in medium-scale panels.

Volcaniclastic deposits in Malinalco

To the east of Malinalco, the Tepoztlán Formation is at least 330 m thick. Two 2D-panels and a detailed stratigraphic section were constructed here (Fig. 3). The sedimentary strata of the section and the two medium-scale panels range in age from 22.8 to 22.1 Ma, and belong to the Malinalco and San Andrés Members of the Tepoztlán Formation.

Large-scale panel 1.1.

Fig. 6 showing large-scale panel 1.1 corresponds to the entire mountain range formed by the Tepoztlán Formation east of Malinalco. Fluvial sediments dominate throughout the entire panel, and are only interrupted by minor intercalated ash-flow tuffs.

Medium-scale panel 1.2.

The base of panel 1.2 (Fig. 7) as well as section MAL (Fig. 8) is characterized by the deposition of at least two thick lapilli-tuff units. There are signs of fluvial reworking and scouring between them. The scours are oriented NW-SE. The top of the stacked tuff layers is marked by the deposition of fluvial sediments. Furthermore, there is an abundance of overlapping channels, laterally with transitions to gravel bars and scours. These sediments are covered by sandy sheet-flood deposits c. 3 m thick before once again predominant overlapping channel-fill elements occur with minor gravel bars. Small, clast-supported lag deposits occur along channel bases and scour surfaces. Channel-fill elements are dominant for the lower half of the panel. In the upper half, the frequency of channel-fill elements decreases and coarse gravel bar elements increase. Throughout the stratigraphy, the gravel bars become coarser and thicker, showing a coarsening- and thickening-upward trend, and are sometimes cut by scours or minor channel elements. Ignimbrites occur at regular intervals of 5 to 15 m. Especially in the lower half, thin (about 5 cm thick) pyroclastic surge deposits can be found below these elements, sometimes with pyroclastic fall layers on top, predominantly consisting of fine pumice lapilli. The upper third of the panel one channel (SSW-NNE orientation) is filled by an ash-flow tuff, followed by 1 m thick lacustrine sediments. The base of the lacustrine sediments is characterized by clayey to silty layers (1 to 5 cm in thickness) that grade into sandy and gravelly layers with a high pumice particle concentration. The lacustrine sediments thin to about 20 cm to the left (NNW) and coarsen. To the left, the stacked

lacustrine sediments are covered by a massive lapilli-tuff, to the right by a sheet-like debris-flow deposit that partly scours the lapilli-tuff.

Stratigraphic section MAL

The Malinalco section (MAL) is located southeast of Malinalco (18.93°N, 99.48°W). It attains a thickness of 93 m (Fig. 8) and can be followed through the medium-scale panel 1.2 (Fig. 7). The section is mainly composed of tuffaceous sandstones and tuffs with minor amounts of clay- and siltstones. The dominant facies are channel-fill and gravel bar elements. Gravel bars increase in abundance towards the top and show a coarsening- and thickening-upward trend. Ash-flow tuffs are prevalent, occurring at regular intervals while pyroclastic surge and fall and lacustrine deposits occur only occasionally.

AMS paleocurrent directions of ash-flow tuffs show a predominant flow direction from SE; few exceptions in the middle of the section show a flow direction from NE. AMS analysis on fluvial deposits show flow directions to the SE, which is consistent with measurements of sedimentary features in this area, showing roughly W-E flow directions.

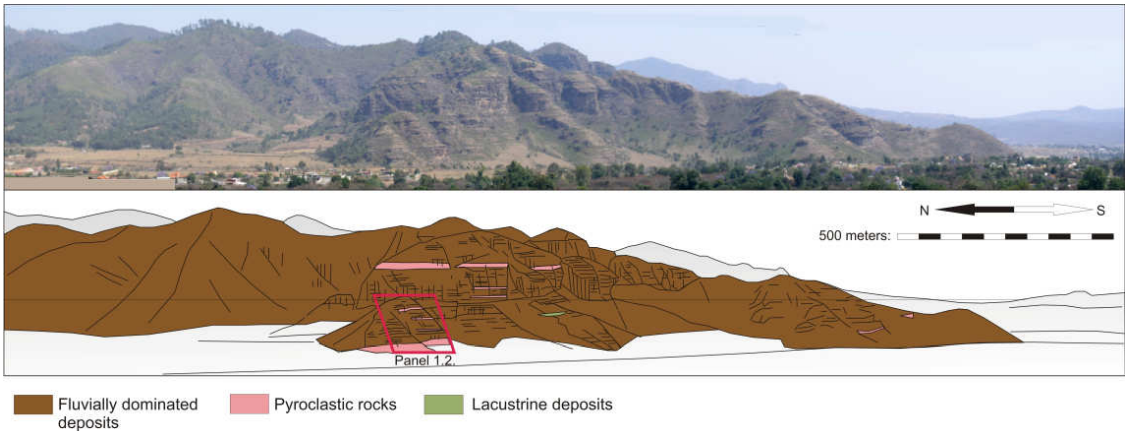

Figure 6. Large-scale panel 1.1. with N-S orientation and a length of c. 2 km. (a) Photomosaic of the study outcrop. (b) Interpretation of the photomosaic. The location of medium-scale panel 1.2. is indicated by the red frame.

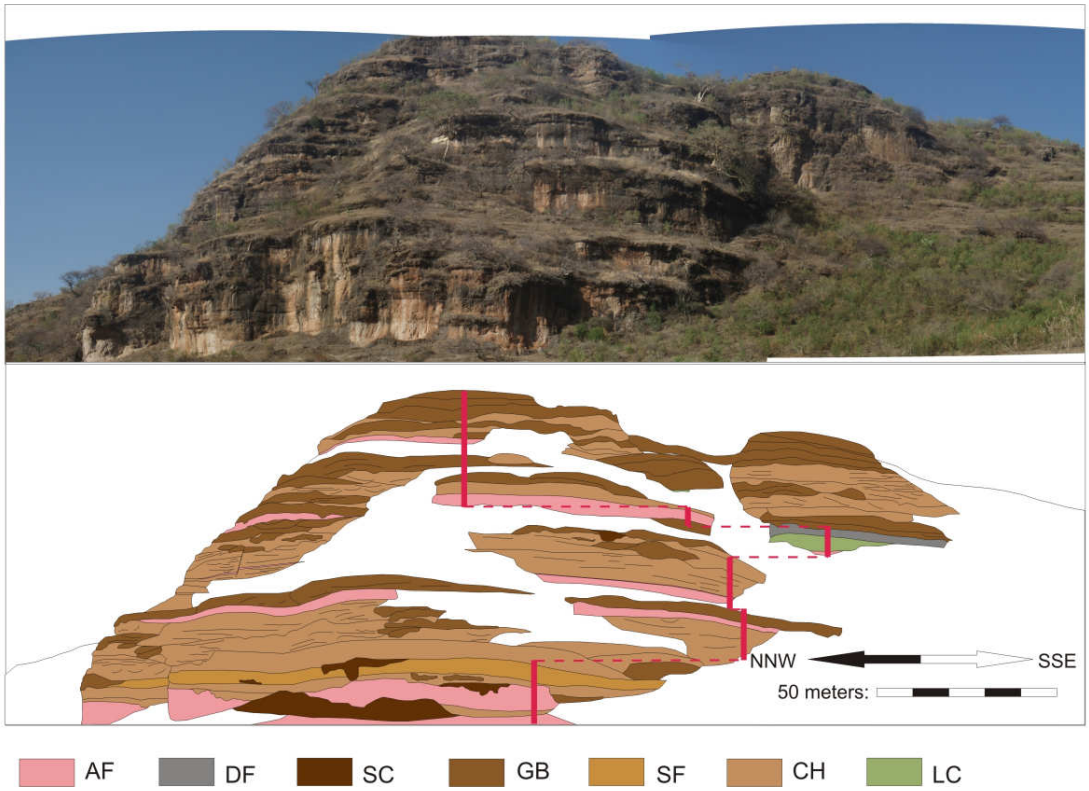

Figure 7. Medium-scale panel 1.2. with NNW-SSE orientation and a length of c. 240 m. (a) Photomosaic of the study outcrop. (b) Interpretation of the photomosaic. The red line indicates the course of the stratigraphic section MAL. AF, ash-flow deposit; SC, scour-fill; GB, gravel bar; SF, sheet-flood deposit; CH, channel-fill; LC, lacustrine.

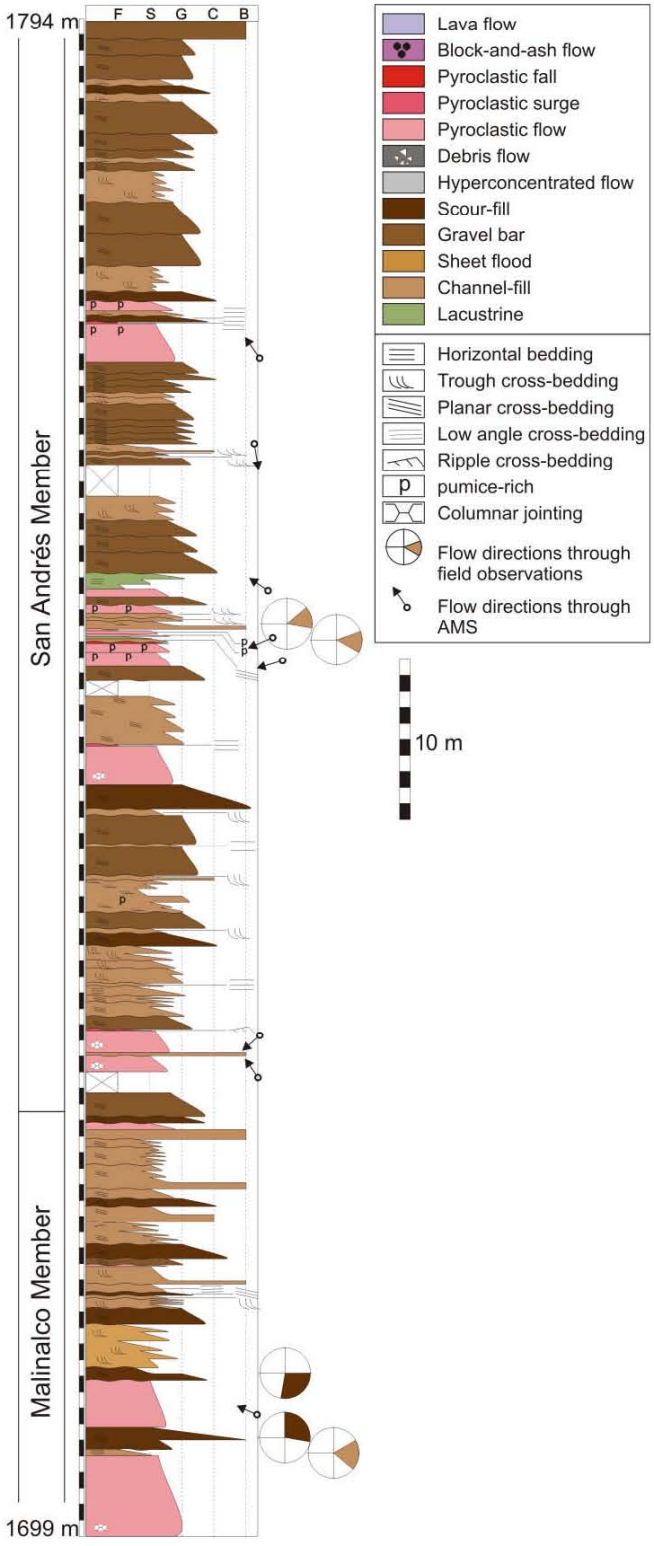

Figure 8. Composite lithostratigraphic section (MAL) of the Tepoztlán Formation near Malinalco

Interpretation

In Malinalco, deposition of the Tepoztlán Formation started with a phase of explosive volcanism, represented by the emplacement of at least two thick (about 5 m) ash-flows at the base of the succession. Signs of scouring by a river and relatively thin fluvial sediments between the flow units indicate that deposition of the ignimbrites took place close to or within a fluvial system that tried to follow its original course between eruptions. The sheetflood deposits on top of these sediments are interpreted to have been formed at the front of a volcanic ring plain, at the transition to the river system and give evidence for deposition in a medial to distal setting, relative to a possible volcanic source. The next 15 m of the succession are dominated by fluvial sediments, indicating a period of relative inter-eruption quiescence. However, the explosive volcanic activity had not ceased completely during this time as indicated by the occurrence of relatively thin (few 10's of cm thick) ash-flow tuffs. Furthermore, the clastic material of the fluvial sandstones and conglomerates is exclusively of volcanic origin. Based on the abundance of amalgamated channels and the continuous upward gradation this part is interpreted to represent an initially high-energy braided stream system, which flowed roughly from west to east. The thickening- and coarsening-upward trends may indicate progradation of the volcaniclastic wedge as deposition from one or more volcanic structures in the vicinity raised depositional slopes (e.g. Smith, 1988). The AMS measurements within the ash-flow tuffs give evidence for two different volcanic sources in the SE and NE, respectively. Previous publications have not identified any volcanoes in the SE. However, in the course of the studies for this paper, a possible volcanic vent area was found in Tlajotlán, c. 9.7 km SE of Malinalco (Fig. 3), characterized by dacitic vent breccias and radial dikes. A possible volcanic source in the NE could be the Zempoala area (c. 20 km from Malinalco), which is supposed to be a major volcanic source of the Tepoztlán Formation (De Cserna & Fries, 1981a) and responsible for 30-400 m thick andesitic lava accumulations near Ahuatenco (Fig. 3).

What is particularly of interest in this location is the development of a lake within the volcaniclastic sediments. The lake is interpreted to have been formed by the deposition of an ash-flow within a fluvial channel that led to the damming of the original river and thus

to a backblock of the stream and the development of a lake (c.f. Manville, 2001). According to Kuenzi et al. (1979) shallow, rapidly infilled lakes of limited lateral extent usually form on aprons due to drainage disruption by lava flows, ignimbrites and landslides, or rapid valley aggradation that impounds tributaries.

The center of the lake is characterized by mostly clayey to silty sediments. Sandy sediments, supplied from NNW direction are inferred to represent the shoreline with a prograding river-delta, similar to a lake-floor fan (Xin et al., 2009) or a Gilbert-type delta (Bestland, 1991; Németh, 2001). Lacustrine deposition was stopped by the accumulation from another ash-flow, which filled the lake basin and was later partly entrained into a subsequent lahar (characterized by debris-flow deposits).

Volcaniclastic deposits in San Andrés

North of the village of San Andrés de la Cal (18.95°N, 99.11°W) the Tepoztlán Formation attains a thickness of about 370 m. Two detailed stratigraphic sections and four 2D-panels were constructed in this area (Fig. 3). The sedimentary strata of the stratigraphic sections range in age from 22.8 to 21.3 Ma, and belong to the Malinalco and San Andrés Members of the Tepoztlán Formation.

Large- scale panel 2.1

The large-scale panel 2.1 shows a part of the San Andrés Member of the Tepoztlán Formation, dominated by tuffs (Fig. 9). The positions of the two stratigraphic sections SA1 and SA2 and the two small-scale panels 2.2 and 2.3 are indicated by red lines and frames.

Stratigraphic sections SAN1 and SAN2

San Andrés section 1 (SAN1), with a thickness of 183 m, is located north of the village of San Andrés (Fig. 10). The lower part of the section is dominated by ash-flow tuffs, gravel bars and minor debris-flow deposits. With increasing height in the succession more and more ash entered the system. Several lobes of a block-and-ash flow deposit can be found

on top of a stack of ash-flow deposits. The upper layer of lapilli-tuff contains gas escape pipes. The top of the section is dominated by ash-flow tuffs and minor amounts of fluvial and debris-flow deposits. The San Andrés 2 section (SAN2), 100 m east of SAN1 attains a thickness of 92 m. The lower and middle part are composed almost entirely of ash-flow tuffs, which can be correlated quite well with strata in SAN1. The top of SAN2 shows an increase in the abundance of fluvial deposits.

Except for four layers, all ash-flow tuffs show AMS paleocurrent directions from the N/ NE. Analyses on fluvial deposits show roughly W-E trending flow directions.

Small-scale panel 2.2

Small-scale panel 2.2 shows a gravel bar dominated depositional system (see Trauth, 2007; Fig. 11) representative of the fluvial sediments in the lower part of the succession. The gravel bar elements at the base of the panel are characterized by planar cross-bedding and thicknesses between 30 cm and 1.3 m. Following these elements, a 20 to 30 cm thick ash-flow tuff can be traced over the entire panel, covered and partly scoured by another stack of gravel bars. A normal fault cuts through the tuff and the gravel bar on top, but does not affect higher gravel bar elements. The right part of the panel is downthrown by about 50 cm. Furthermore, a well rounded dacitic ballistic block of 2.5 m in diameter can be found next to the fault. The layers below the block show bomb sag structures.

Small scale panel 2.3

Representative of the ash-flow tuff-dominated part of the Tepoztlán Formation, panel 2.3 shows a succession of several ash-flow, surge and fall deposits (see Trauth, 2007; Fig. 12). A basal thick ash-flow deposit is followed by a succession of stacked pyroclastic surge accumulations, showing signs of erosion in the left and right part of the panel. Especially in the right part, this erosion was caused by the development of a fluvial channel as indicated by remnants of sandy channel-fill elements. Rip-ups of the pyroclastic flow deposit occur within the fluvial sediments. The fluvial channel is filled by a stack of three ash-flow tuffs. Simultaneously, a fall layer can be traced throughout large parts of the panel but was partly eroded by subsequent pyroclastic flows. On top of

this stack, a very pumice-rich ash-flow tuff can be traced over the entire panel, followed by at least two more thick, lithic-rich ignimbrite sheets.

Large scale panel 2.4

Panel 2.4 (Fig. 13) has a S-N orientation, showing the Tepoztlán Formation at the eastern side of the mountain range north of San Andrés. While sandy channel elements and gravel bars dominate in the south, sheet-flood deposits intervene from the north and are followed by debris-flow deposits, which rarely reach the southern edge of the panel. Ash-flow tuffs are abundant throughout.

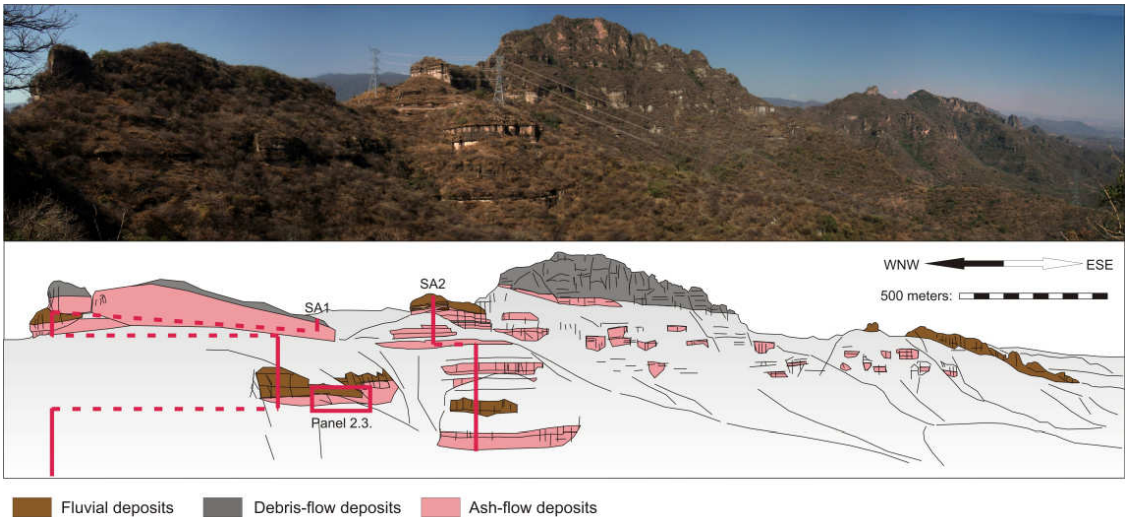

Figure 9. Large scale panel 2.1. with WNW-ESE orientation and a length of c. 4 km. (a) Photomosaic of the study outcrop. (b) Interpretation of the photomosaic. The red lines indicate the courses of the sections SAN1 and SAN2. The location of small-scale panel 2.3. is indicated by the red frame.

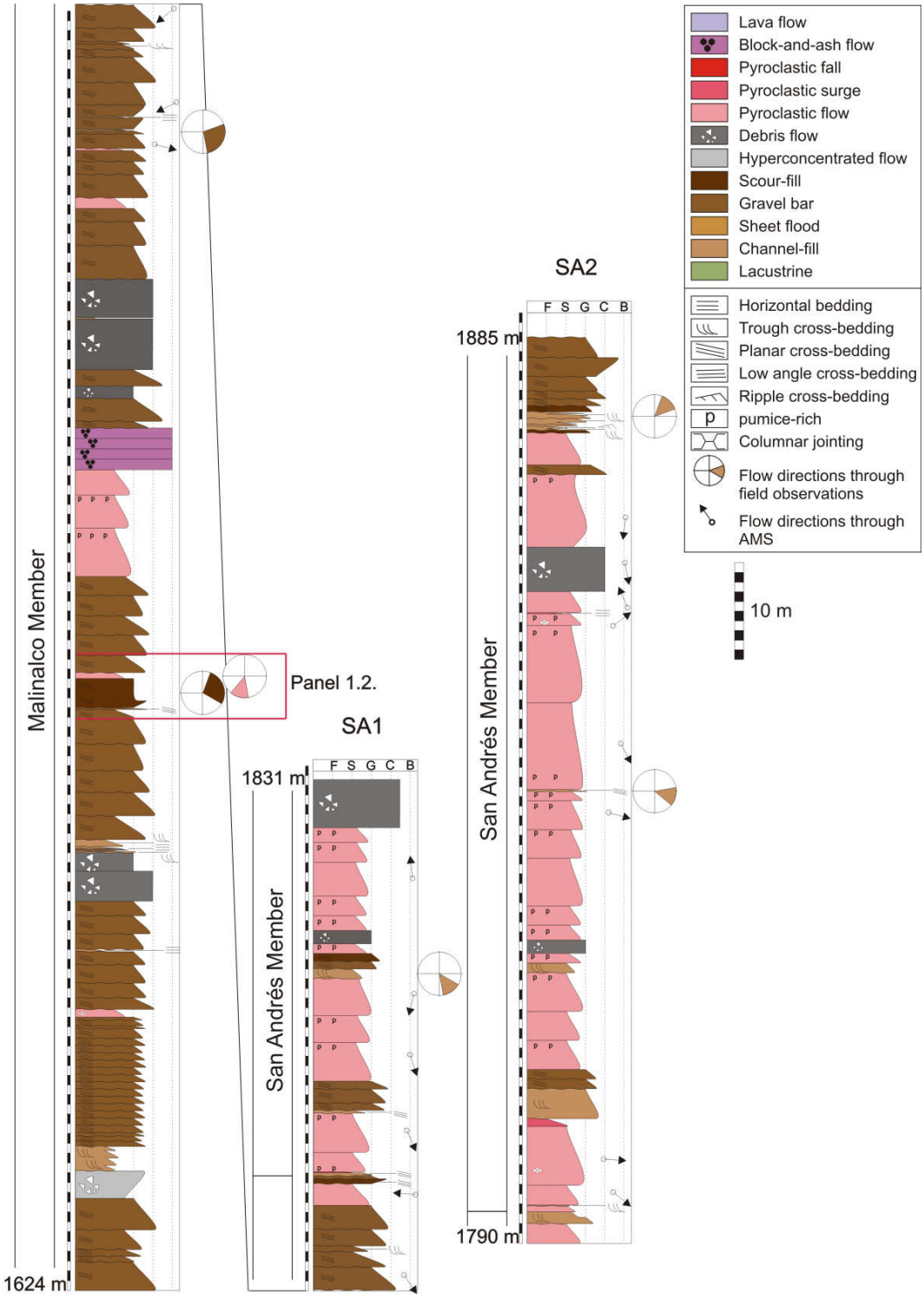

Figure 10. Composite lithostratigraphic sections SAN1 and SAN2 of the Tepoztlán Formation near San Andrés. The location of small-scale panel 2.2. is indicated by the red frame.

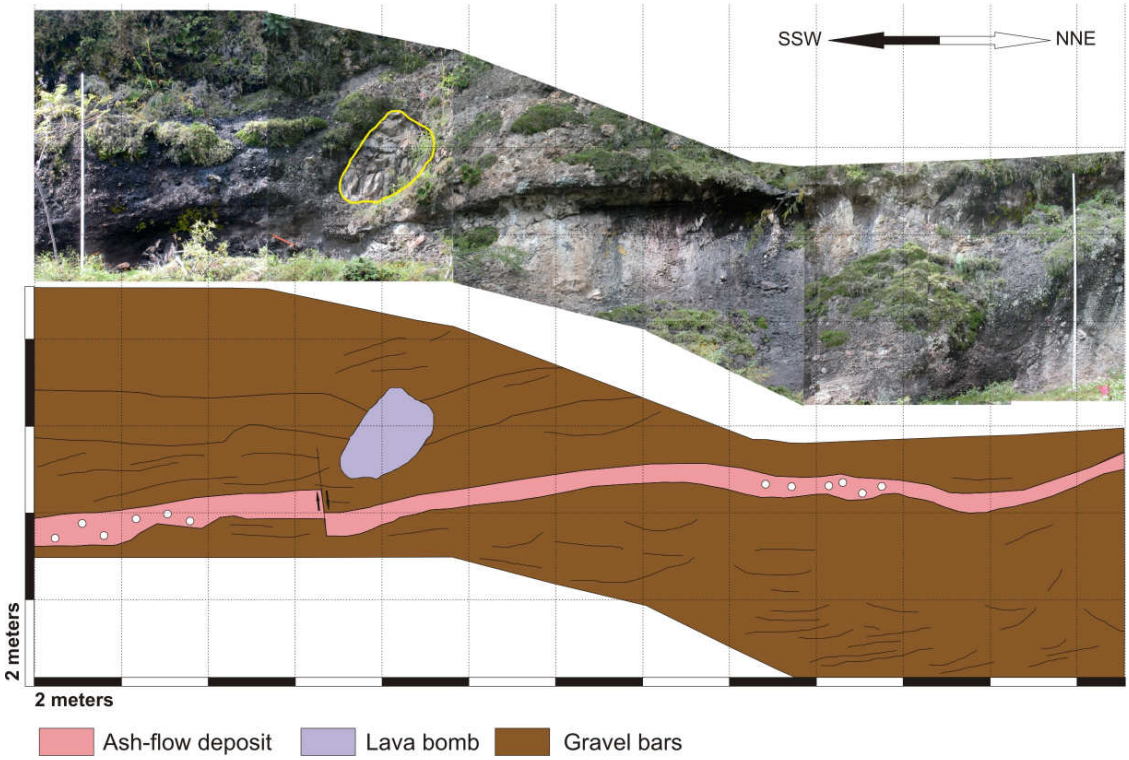

Figure 11. Small scale panel 2.2. with SSW-NNE orientation and a length of c. 25 m. (a) Photomosaic of the study outcrop. (b) Interpretation of the photomosaic (from Trauth, 2007).

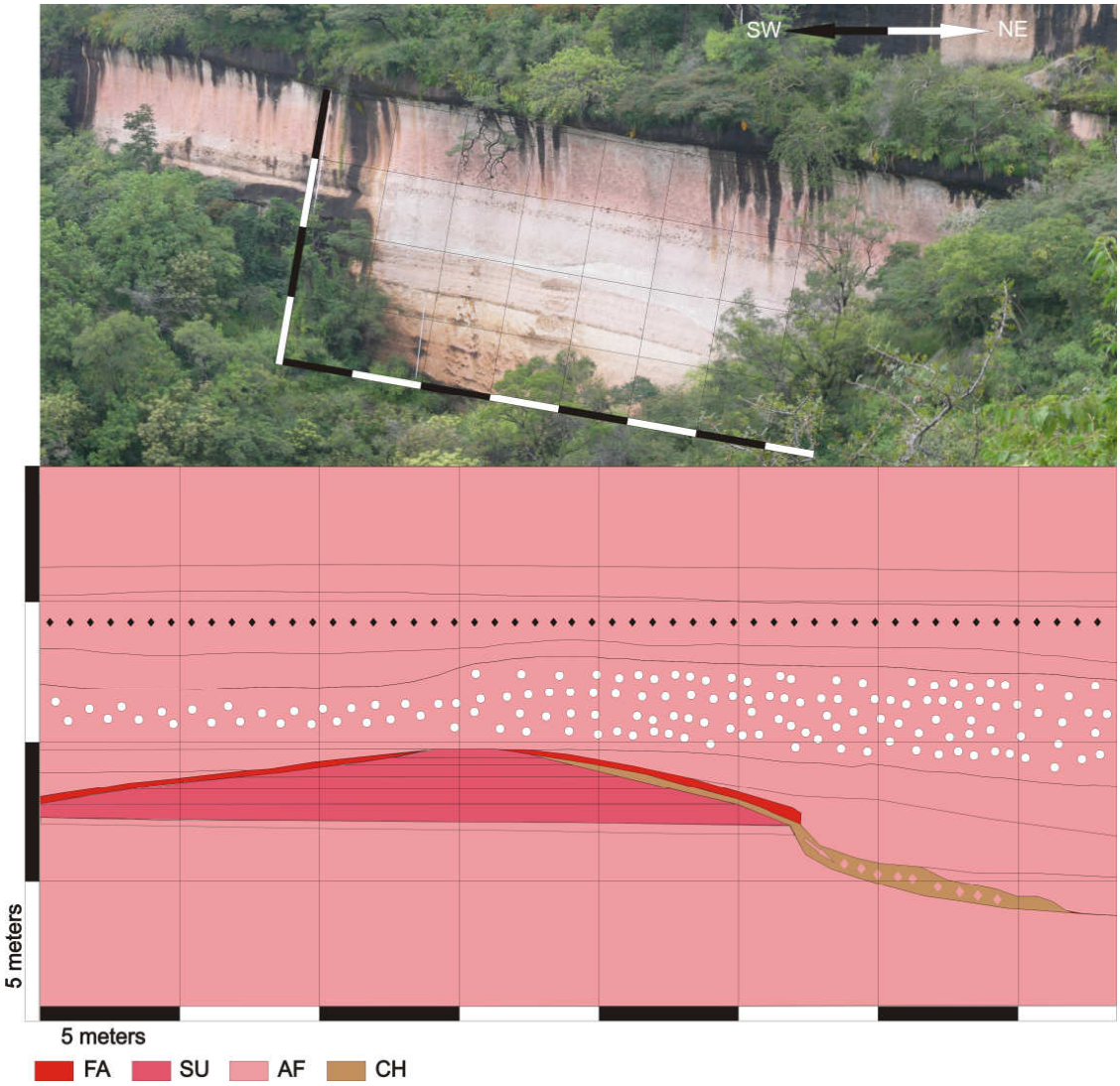

Figure 12. Small scale panel 2.3. with SW-NE orientation and a length of c. 39 m. (a) Photomosaic of the study outcrop. (b) Interpretation of the photomosaic. FA, pyroclastic fall deposit; SU, pyroclastic surge deposit; AF, ash-flow deposit; CH, channel-fill (from Trauth, 2007).

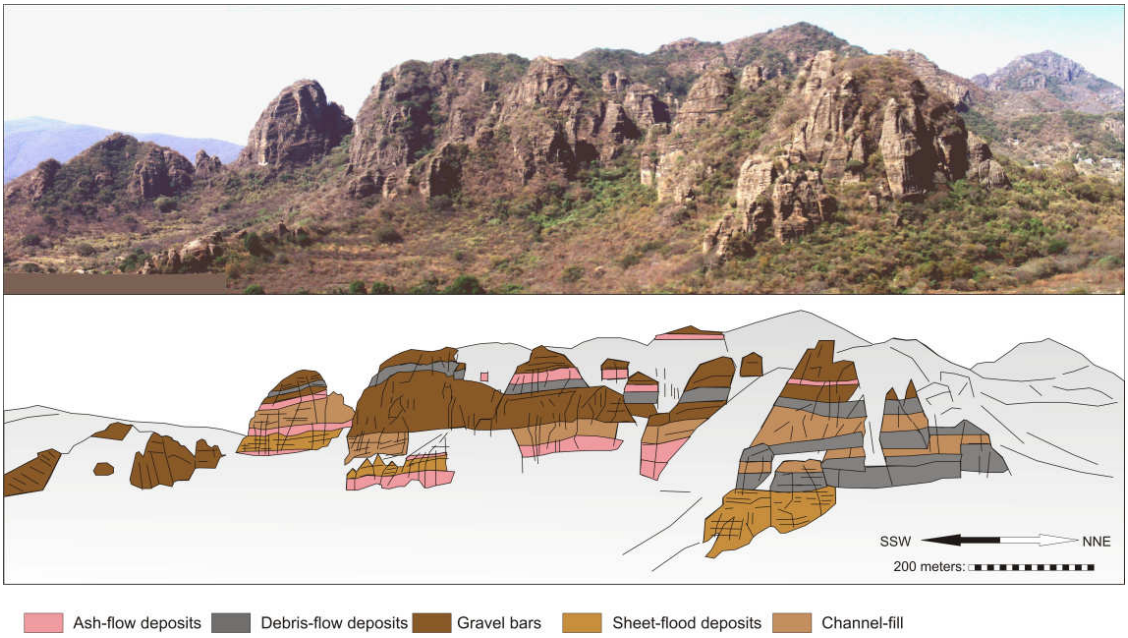

Figure 13. Large scale panel 2.4. with SSW-NNE orientation and a length of c. 2 km. (a) Photomosaic of the study outcrop. (b) Interpretation of the photomosaic.

Interpretation

The lower part of the succession at the base of section SAN1, i.e. the oldest exposed deposits of the Tepoztlán Formation within the study area is characterized by sandy channel-fills and gravel bars with single intercalated mass-flow deposits, ranging from accumulations of hyperconcentrated flows to debris flows. Orientations of imbricated gravels, scour walls and mapped paleochannels indicate that a fluvial transport direction from west to east was dominant with a vaguely radial dispersal pattern. The predominance of low-angle erosional surfaces, small bouldery gravel bars, and flat-bedded to cross-bedded, tuffaceous sand supports deposition in a system of shallow migrating channels with longitudinal bars, diffuse gravel sheets, and unstable banks. Based on the abundance of overlapping channels and the continuous upward gradation this part is interpreted to represent a braided stream system (c.f. Smith, 1987). Small, clast-supported lag deposits occur along channel and scour bases. The coarse-grained volcanic debris was probably transported to the area by debris flows, but only scoured remnants can be noticed in the lower part of section SAN1.

The outcrops of bedded, reworked tuff along with the accumulation of debris-flow and stream deposits in broad, shallow channels suggest deposition in a moderately aggradational setting of low relief. In the middle part of section SAN1 stacked layers of orange to pink, lithic-rich lapilli-tuff as thick as 11 m belong to the oldest primary volcaniclastic material and give direct evidence for explosive activity. Vertical gas-escape structures are common in these deposits. They are covered by several successive layers of tuff breccia, which are interpreted to originate from block-and-ash flows. Their emplacement was followed by immediate or subsequent downstream dilution by the stream water, ending up as hot or cold “laharic” currents, depositing debris flow units. Locally, interstratified lava flows give evidence for effusive eruptions and were the dominant source for the volcanic detritus preserved in the sections.

On top of the lava flows, another 40 m-thick package of amalgamated and stacked gravel deposits is exposed with minor intercalated pyroclastic flow deposits.

The vertical transition from sandy deposits to thicker conglomerates reflects a change in the fluvial architecture. The fluvial patterns are characterized by a coarsening- and thickening-upward trend and thus an increase of incorporated primary volcanic material, pointing to progradation or increasing volcanic intensity in the volcanic source area. This hypothesis is supported by the occurrence of near-vent block-and-ash-flows and abundant ash-flow tuffs that are increasingly abundant towards the upper part of the succession, suggesting a progressive progradation of the volcanic system. The tops of section SAN1 and section SAN2 are clearly dominated by massive lapilli-tuffs originating from ash flows and recording a major explosive eruption phase. Early ash-flow deposits are still strongly confined to paleovalleys with a N-S to NNW-SSE orientation, suggesting a supply of material from point sources in the north. One example for these paleovalleys can be seen in panel 2.3 where a fluvial valley (50 m width) was filled by several tuff layers, originating from ash-flows and pyroclastic surges. The succeeding tuff layers however, have sheet-like appearances, indicating a smoothing of the depositional surface after the filling of the channel, which allowed subsequent flows to produce sheet-like deposits. N-S to NNW-SSE flow directions are also indicated by AMS analyses on ash-flow tuffs, showing that AMS trends tend to mirror local stream valleys or slope directions (Fisher et al., 1993) and thus the paleotopography of the ancient ring plain.

Divergent data from the N-S/ NNW-SSE directions, however, show a W-E or E-W direction, i.e. parallel to the suspected braided river valley that drained the volcano. This suggests that much of the material flowed radially off the outer slopes of the ring plain irrespective of the direction from the original source area (e.g. Fisher et al., 1993). Well preserved organic matter (plant debris and palynomorphs) within the pyroclastic material points to relatively low depositional temperatures below 350°C (Stach et al., 1982). The top of the sequence again shows an increase in fluvial material. Furthermore, debris-flow deposits in the form of pumiceous diamicts, introduced from the north are another indication for increasing influence by a possible source in that area. This is documented by panel 2.4 (Fig. 13), showing the interfingering and successive progradation of the volcanic ring plain into the underlying braided-river system.

An indication of synsedimentary tectonic activity is the normal fault in 2.2, which may have formed during an earthquake due to volcanic activity. The block next to the fault is interpreted to present a volcanic bomb. The distribution of very large particles is generally restricted to a few kilometres from the vent (Orton, 1996). By means of the bomb sag structures a flight direction from NNE to SSW can be proposed, giving more evidence for a possible volcanic source in the north.

Volcaniclastic deposits in Tepoztlán

North of Tepoztlán (18.99°N, 99.10°W) the thickness of the Tepoztlán Formation is about 380 m. One detailed stratigraphic section and one 2D-panel were constructed in this area (Fig. 3). The volcanic and sedimentary strata of the stratigraphic sections range in age from 21.8 to 18.8 Ma, belonging to the San Andrés and Tepozteco Member of the Tepoztlán Formation.

Large scale panel 3.1

Panel 3.1 (Fig. 14) shows a change from a prevailing conglomerate and cross-bedded sandstone facies in the lower half of the panel to a mainly diamict lithofacies in the upper half, documenting the change from fluvial-dominated to a mass flow-dominated

sedimentation within the Tepoztlán Formation sedimentary succession. The course of the stratigraphic section TEP is indicated by the red line.

Stratigraphic section TEP

The Tepozteco section (TEP) is located north of Tepoztlán (Fig. 15). The thickness of this section is 378 m. The lower part is dominated by tuffaceous sandstones and conglomerates resulting from gravel bars and sandy channel fillings. Minor amounts of the massive tuff breccia lithofacies, deposits of at least two block-and-ash flows, can be recognized. The upper two-thirds of the section are dominated by the deposition of coarse tuffaceous diamicts, i.e. debris-flow deposits resulting from lahars (e.g. Rodolfo & Arguden, 1991). It was not possible to ascertain the number of debris-flow deposits in the vertical sequence because distinct changes in sedimentology or erosional contacts were not apparent. Lapilli-tuff facies is only a minor constituent in this part of the section. The sedimentary succession is locally capped by a 20 m-thick dacitic lava flow. The top of the stratigraphic section is represented by more debris-flow deposits with minor amounts of cross-stratified tuffaceous sandstone.

AMS analyses on lava as well as fluvial deposits point to a roughly N-S-trending flow direction. AMS directions from fluvial deposits are supported by analysis of sedimentary paleocurrent structures, showing the same direction of transport.

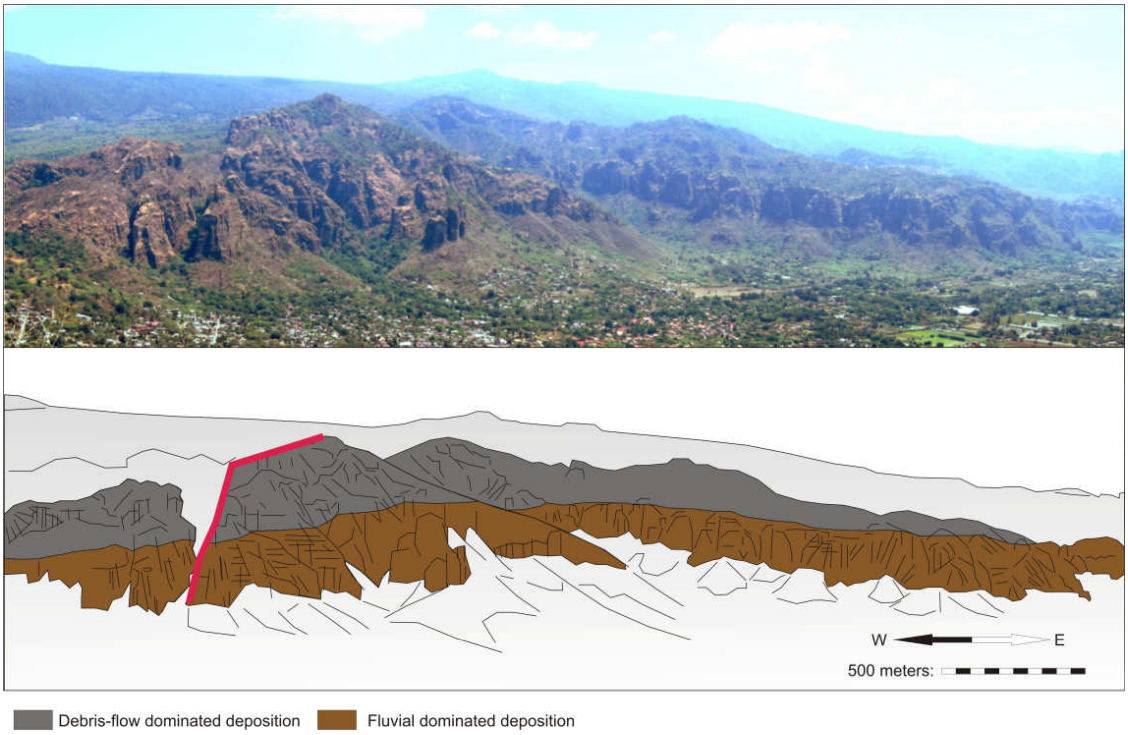

Figure 14. Large scale panel 3.1. with W-E orientation and a length of c. 4 km. (a) Photomosaic of the study outcrop. (b) Interpretation of the photomosaic. The red line indicates the course of the stratigraphic section TEP.

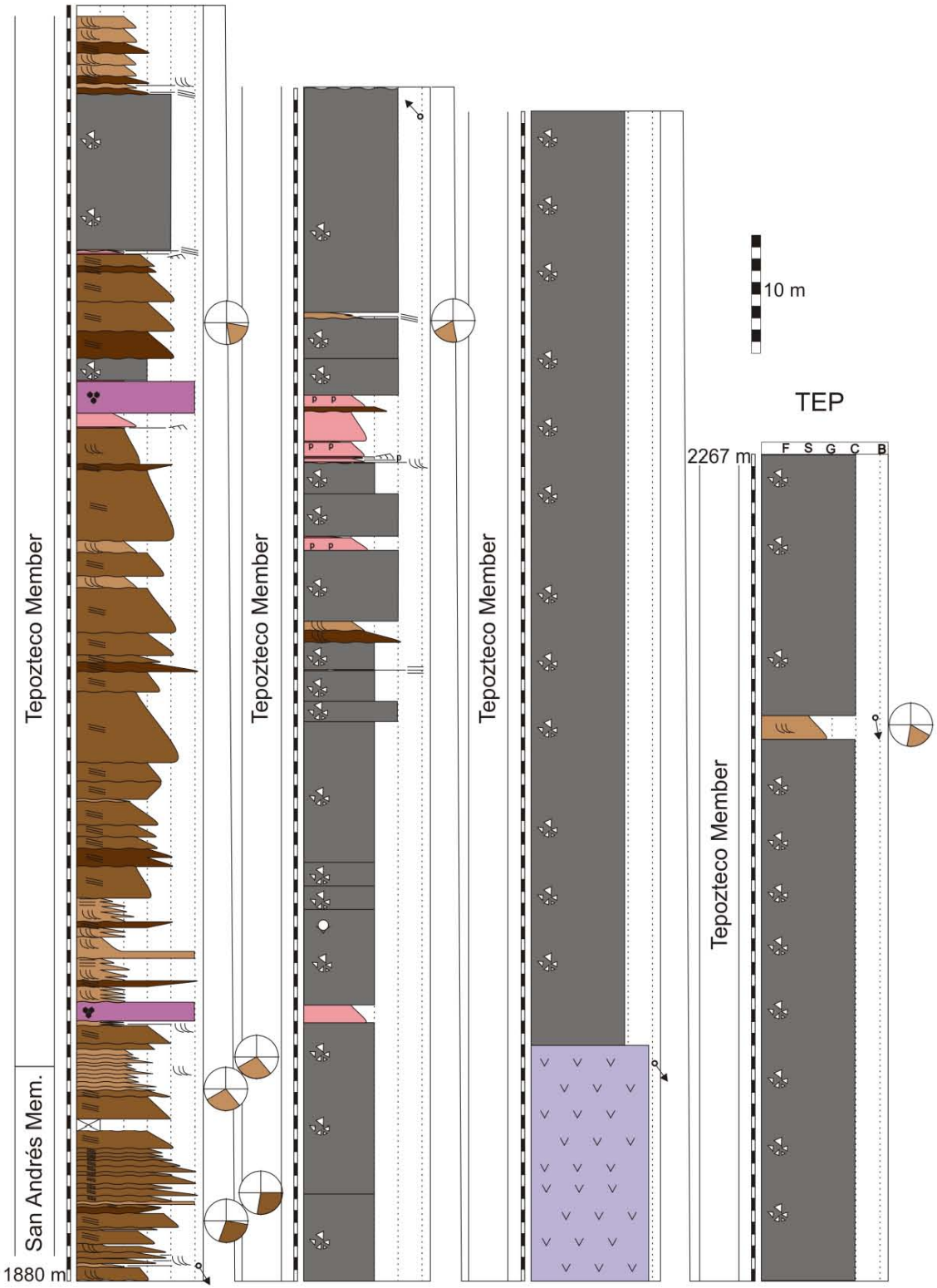

Figure 15. Lithostratigraphic section TEP of the Tepoztlán Formation near Tepoztlán (for legend see Fig. 10).

Interpretation

The characteristics of the sedimentary facies and bed geometry in the lower part of the sedimentary succession of the Tepoztlán Formation, documented in this location, indicate that the system was dominated by streamfloods of high enough competence to transport even boulder-size clasts. The predominance of low-angle erosional surfaces, small bouldery bars, and relatively thin sandy channel-fills supports deposition in a system of shallow migrating channels with longitudinal bars and unstable banks, characteristic of a braided river system. Bouldery conglomerates at the base of channels are interpreted to be lag deposits. All clasts within the fluvial deposits are of volcanic origin. The sandy matrix is probably due to reworking of unlithified ash. This shows that volcanic activity was still ongoing within the study area and regularly introduced fresh, unlithified volcanic material into the stream. The relatively thin pyroclastic-flow deposits are direct evidence for volcanic activity. Up-section, the fluvial sediments are suddenly replaced by a massive stack of laharic debris-flow deposits, which dominate the sedimentary succession to the top. The debris flows are inferred to have been produced by relatively near-source reworking of vent-facies pyroclastic material. The abundance of channelized to unchannelized debris-flow deposits is commonly indicative of small coalescing alluvial-fans with high angles of repose and restricted catchments (Nemec & Postma, 1993). According to Ferruci et al. (2005) a minimum topography is necessary for the formation of debris-flows, which is distinguished in three sectors: 1) a water supply zone (slope > 32°) where rain water is enriched in mud and concentrated in the initiation zone; 2) an initiation zone (or source area *sensu stricto* slope with ~30°) where debris flows form and; 3) a transport and deposition zone where debris flows deposit levees and terminal lobes (slope ~30°).

The lack of fluvial sediments suggests that post-depositional fan incision was limited. The volcaniclastic sequence is capped by a thick dacitic lava flow, suggesting a brief decrease in eruption intensity and a transition from explosive to effusive activity. The succession is completed by the deposition of further debris-flow deposits. This could point to renewed explosive volcanic activity and immediate reworking of fresh pyroclastic material by mass flow processes, leaving no trace of primary deposits.

Another, probably more accurate explanation for the huge packages of mass-flow deposits could be deposition during a phase of edifice destruction (c.f. Zernack et al., 2009) and thus the final stage within the evolution of the Tepoztlán Formation.
Similar to location SAN, analysis on AMS and sedimentary features imply N-S to NNW-SSE flow directions, following the paleotopography of the ancient ring plain with a supposed source in the north. Although there are no visible signs for a volcanic vent area because of a thick cover of Pliocene to historic lava flows, the Sierra Chichinautzin volcanic field (c. 5 km away) is the most probable candidate location for a proto-edifice supplying material for the Tepoztlán Formation.

DISCUSSION AND EVOLUTIONARY MODEL

The vertical and lateral analysis of individual lithofacies types and their distribution within the study area, as well as information gained during mapping in the field and outside the stratigraphic sections, can be integrated in three depositional models, forming a concise evolutionary model of the Tepoztlán Formation (Fig. 16), and illustrating their importance for the interpretation of the succession. The facies patterns within the stratigraphic sections record temporal changes in sedimentation, showing syn- and inter-eruptive sedimentation as indicated by primary and secondary volcaniclastic and fluvio-lacustrine depositional processes. The interpretation of these facies patterns also reveals post-eruptive volcaniclastic resedimentation in a fluvial environment, intertwining with sedimentation from at least three partly coalescing volcanic ring plains during and in the aftermath of explosive eruptions. Volcanic activity, combined with minor syndepositional tectonics, were the main controlling factors in alluvial sedimentation. During episodes of increasing sediment supply by volcanic activity, progradation of the ring plains was recorded and coarsening-upward trends developed. Intervals of quiescence separating eruptive periods are characterised by landscape re-adjustment, accompanied by deposition of fluvial and lacustrine sediments (c.f. Zernack et al., 2009).
The locations of volcanic edifices were deduced either through direct observations in the field or indirectly, based on lithofacies associations and by means of sedimentary

paleocurrent and AMS measurements. Furthermore, the course of the braided-river system outside the documented and measured stratigraphic sections is considered to be more or less schematic. Inflows from the north are supposed to have been present at that time, considering that the Valley of Mexico was drained to the south (Ochoterena, 1978), but could not be identified in the field.

Once the lithofacies and their distribution had been identified, analyzed and interpreted, and the paleocurrent directions had been investigated, three distinct paleoenvironmental settings could be deduced, characterized by the three members of the Tepoztlán Formation during the Lower Miocene: (1) the Malinalco Member, a setting dominated by the deposition from a braided river system, (2) the San Andrés Member, a setting dominated by volcanic edifice development, and (3) the Tepozteco Member, a setting dominated by volcanic edifice destruction.

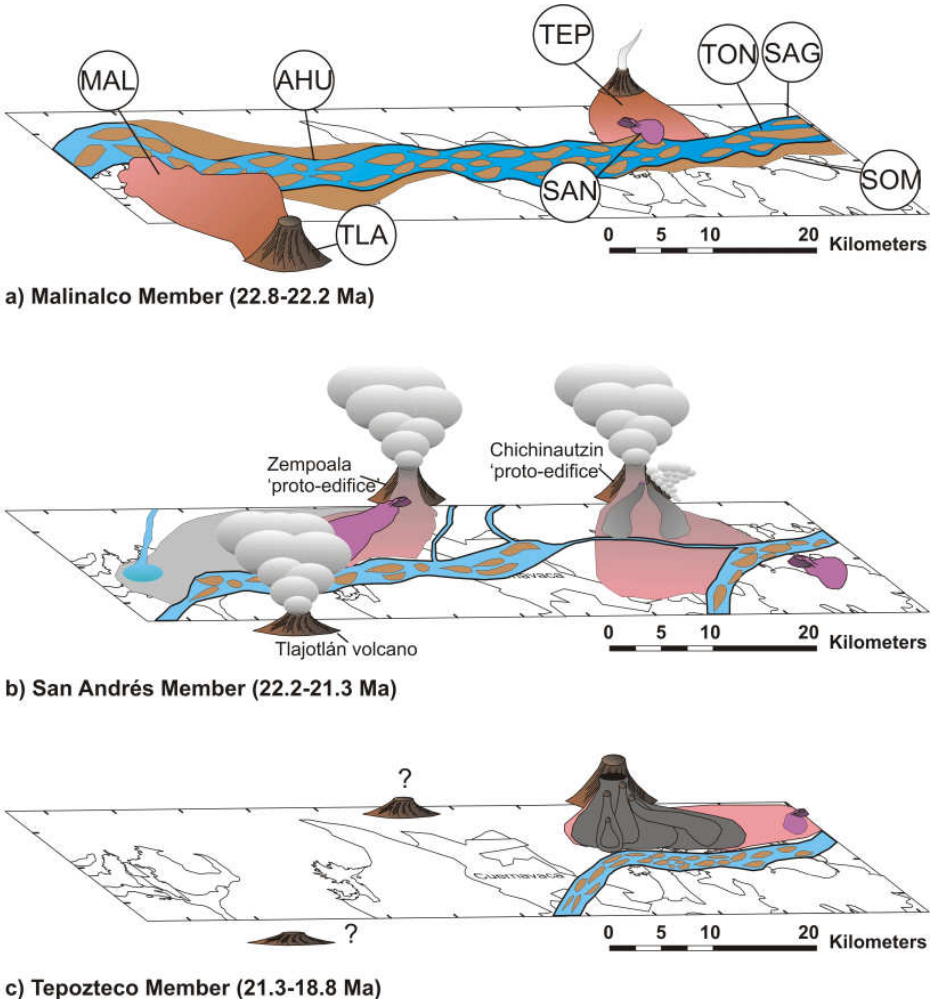

Figure 16. Paleoenvironmental reconstruction of the three distinct depositional settings: a) braided river setting (Malinalco Member, 22.8-22.2 Ma), b) volcanic edifice construction (San Andrés Member, 22.2-21.3 Ma), and c) volcanic edifice destruction (Tepozteco Member, 21.3-18.8 Ma). MAL – Malinalco; TLA – Tlajotlán; AHU – Ahuatenco; SAN – San Andrés; TEP – Tepozteco; SOM – Cerro Sombrerito; TON – Cerro Tonantzin; SAG – San Agustín.

Braided river setting (Malinalco Member, 22.8 - 22.2 Ma)

The studies on sedimentary features and paleocurrent directions show that a W-E trending braided river system dominated the study area between 22.8 and 22.2 Ma. The fluvial sediments, mostly gravel bars and sandy channel-fills, were predominantly

deposited near Malinalco, Ahuatenco and San Andrés. Vertical stacking of sand and gravel bodies are interpreted to be due to aggradation with shifting of channel bars associated with channel switching (e.g. Bridge, 1993). The complete lack of paleosols and non-volcanic clasts gives evidence for an already active system with frequent eruptive activity and immediate subsequent reworking and resedimentation. Small-scale pyroclastic eruptions, mainly depositing close to the vent, supplied relatively small to moderate rock volumes (c.f. Platz et al., 2007) that were entrained into the axial fluvial system. SE of Malinalco a volcanic center of this time could be identified by vent breccias and radial dikes (18.52°N, 99.23°W). The AMS measurements on pyroclastic rocks in Malinalco are consistent with this source region. According to paleocurrent data taken from the San Andrés sections (SAN1+2) another volcanic center must have existed in the area of the present day Sierra Chichinautzin, north of Tepoztlán.

Following the eruptions, volcaniclastic debris was reworked from proximal areas and discharged into the basin. This resulted in the development of a low-sinuosity channel system with high-sediment-laden hyperconcentrated flows after heavy rains. Debris-flows produced during this period were probably restricted to proximal areas due to the lower elevation of the source area (c.f. Zernack et al., 2009). However, the relatively thin, tabular, hyperconcentrated-flow deposits are interpreted as dilute end-members of debris flows (Pierson, 2005) and to mark the transition from the ring plain to the braided river system. The prevalence of clasts of intermediate composition and of large size is consistent with a limited distance from the source via a high-energy transport system and thus suggests contemporaneous volcanism and sedimentation. The overall coarsening- and thickening-upward trend, together with an increase in average grain size, can be attributed to growth of the stratovolcanoes and the progradation of large fan lobes of the ring plain systems into the river basin (e.g. Clemente & Perez-Arlucea, 1993; Horton & DeCelles, 2001; Uba et al., 2005).

Volcanic edifice construction (San Andrés Member, 22.2 - 21.3 Ma)

During the deposition of the San Andrés Member a further progradation of the volcanic system is recognized, combined with a sudden increase in volcanic activity, which is associated with the deposition of massive ignimbrites and the most voluminous lava flows of the Tepoztlán Formation. The lower part of the San Andrés Member, especially in Malinalco, is still dominated by the deposition of thick horizons of gravel bars and sandy channel-fills, indicating the on-going sedimentation of the axial braided river system. Subsequently, medial accumulation of the ring plain is characterized by massive sequences of lapilli-tuff beds with intercalated debris-flow and hyperconcentrated-flow deposits. These are sheet-like or confined to channels where the landscape has been incised by rivers and streams (c.f. Procter et al., 2009). In the beginning, pyroclastic material filled up the existing fluvial channels, explaining their lens-shaped appearance. Lacustrine sediments found in Malinalco and near the village of Santo Domingo (19.00°N, 99.03°W) point to the development of lahar-dammed lakes after partial covering of the former river bed by volcanic activity and a ponding of the water in the newly formed sedimentary basin (c.f. Kuenzi et al., 1979; Manville, 2001). In San Andrés, the pre-existing fluvial system was partly covered or diverted by volcanic deposits and could only follow its original course in times of quiescence, as indicated by thin fluvial sediments within the thick sheets of ignimbrites. Explosive eruptions from small, andesitic-dacitic composite volcanoes, causing the deposition of pyroclastic flows and subordinate pyroclastic surges, were accompanied by few effusive episodes. The eruptive events generated only few ash falls and relatively small-volume or small-runout pyroclastic density currents, probably extending not more than 20-30 kilometers from their vents. Although initial plinian eruption clouds may have developed, they would have been short-lived and collapsed early into an ash and debris fountain, which fed pyroclastic flows onto the outer slopes. This may explain the existence of only few fall deposits (e.g. White & Robinson, 1992). Another explanation could be that the eruptions were dominated by dome-forming effusive activity producing block-and-ash flows and lava flows, but only a few large plinian eruption columns and thus little distal tephra. One example of this eruptive style is Mount Unzen, Japan, which is characterized by effusions of thick lava flows and/or lava domes associated with gravitationally driven block-and-ash-flow deposits (Hoshizumi et al., 1999; Ui et al., 1999). Explosive eruptions of

vesiculated pumiceous materials are very rare (Hoshizumi et al., 1999). The block-and-ash flows within the Tepoztlán Formation were repeatedly generated upon collapse of gravitationally unstable outflows from the growing lava domes either in the summit crater itself or from peripheral domes. Dome building events commonly occur at many stratovolcanoes between combined stages of cone building separated by cratering and collapse events (Carrasco-Núnez, 1999). Few large plinian eruptions then produced ash flows that moved down the slopes of the volcano. It can be assumed that at least intermittent fallout must have occurred, especially at the beginning of the eruptions. This loose material must have been continuously stripped by subsequent rain, lahars, and pyroclastic flows (c.f. Siebe et al., 1993). Rowley et al. (1981) report ash fall deposits, several cm thick, adjacent and on top of the June 12, 1980 pyroclastic-flow deposits at Mount St. Helens. These fine beds were completely eroded and did not last for more than a few weeks. The same is reported by Rose et al. (2008) about the October 14, 1974, tephra deposit from Volcan de Fuego, Guatemala. The fine-grained, generally thin tephra deposits, commonly produced by dry subplinian eruptions of many composite volcanoes, are described as short-lived and seem to have disappeared due to erosion after few weeks. Interbedded fluvial sediments represent local re-establishment of the paleostream and fluvial reworking in the course of landscape adjustment. However, no paleosoils have been recorded, indicating relatively short inter-eruption periods. Later, primary deposits have a sheet-like appearance, covering and modifying the paleotopography and leading to further steepening of the relief in the context of the growing ring plain system in the north. Regionally, the thickest ignimbrites can be found near San Andrés (up to 30 m) while thick lava flows are prevalent in the vicinity of Tlayacapan and Ahuatenco (up to 400 m). Similar to the Malinalco Member, AMS measurements on the ignimbrites in San Andrés suggest a point source in the present-day Sierra Chichinautzin, where the proto-edifice is supposed to be buried below modern lava flows. In Malinalco, AMS measurements on relatively thin ignimbrites point to a volcanic source in the NE, deviating from the formerly described source in the SE near present-day Tlajotlán and thus suggesting the coalescing of the ring plains of two different volcanoes in this location. The most probable volcanic source in the NE of Malinalco is the present-day Zempoala complex (Fries, 1960), which was suggested by De Cserna & Fries (1981a) to

be one of the major source areas of the Tepoztlán Formation in Malinalco. The Zempoala volcanic region is furthermore supposed to be the source of the massive lava flows, which can be found near Ahuatenco (K/Ar ages of 22.4±0.5 Ma, 21.9± 0.5 Ma; Lenhardt et al., 2010). Here, the lava, normally reaching thicknesses of 30 m, flowed southward into a pre-existing depression, reaching a maximum thickness of 400 m. The top of the San Andrés Member is characterized by further progradation of the ring plain, indicated by an increase in sheet-like lahars.

Volcanic edifice destruction (Tepozteco Member, 21.3 - 18.8 Ma)

The deposition of the Tepozteco Member is characterized by sedimentation in the eastern part of the study area (Tepoztlán and Tlayacapan region). In contrast, deposition in the west (Malinalco and Ahuatenco region) is missing and seems to have ceased during that time. This is either due to a shifting of the initial braided river system during that time, combined with a cessation of volcanic activity of the Tlajotlán and Zempoala volcanic center, or a later erosion of younger sediments. However, in the other parts of the Tepoztlán Formation, deposition was still prevalent. Paleocurrent data on sediments indicate that basin sedimentation underwent a significant change from a predominant W-E trending fluvial to a N-S trending mass-flow depositional system. The influence of the ring-plain, which could already be observed within the Malinalco and San Andrés Members, increased and overcame the formerly dominant axial fluvial system during this period. This can be well seen within the TEP section, which is interpreted as the active part of the volcanic ring-plain, presumably developing at the southern edge of a prominent volcanic edifice with an estimated altitude exceeding 3000 m above sea level (Lenhardt, 2009). Similar to the two members described before, paleocurrent analysis and lithofacies associations suggest a volcanic source area in the north, buried below the modern lava flows of the present-day Sierra Chichinautzin, about 5 km away from Tepozteco. Clast compositions and lithologies indicate that all material was locally derived. Deposits originating from debris flows are inferred to have been produced by relatively near-source reworking of pyroclastic material. The association of thick lavas

(up to 20 m), pyroclastic breccias, and bouldery lahar deposits as can be seen in section TEP is common on the flanks of stratovolcanoes and characterize many proximal to median apron settings (e.g. Vessel & Davies, 1981; Mack & Rasmussen, 1984; Hackett & Houghton, 1989). Throughout the section TEP, the amount of primary volcaniclastic products is decreasing and is absent in the upper third while debris flow deposits are increasing in number and thickness, suggesting a growing height and volume of the edifice (c.f. Zernack et al., 2009). The end of sedimentation within the Tepoztlán Formation is characterized by edifice destruction of the prevalent volcano complex in the north, which generated various types of debris-flow deposits. This destructional phase can be due to the volcanic edifice reaching its critical point at which its structure becomes sufficiently unstable (c.f. Zernack et al., 2009). Normally, a volcanic cycle is closed with a major sector or cone collapse, represented by an increase in debris avalanches and debris flows in medial areas (c.f. Zernack et al. 2009; Procter et al., 2009). Direct evidence for a major collapse of the volcanic edifice such as debris avalanche deposits is absent in the studied sedimentary succession, most probably due to the distance from the source and possibly erosion. However, it can be assumed that debris flows developed from proximal avalanche areas and possible scarp and debris avalanche deposits (Procter et al., 2009). The increase in sediment supply, associated with high rates of lahar activity, resulted in an aggradation in stream valleys and on aprons surrounding the volcanic edifice (c.f. Vessel & Davies, 1981; Scott, 1985; Smith, 1987). The lahars flowed southward from their source area and spreaded over the braided stream valley, leading to a partial covering or southward shift of the initial braided river system. Initially confined lahars that are recorded in lower parts of section TEP are due to incised topography, as it is the case at most volcanoes in the Cascades, e.g. Mt. Rainier (Vallance & Scott, 1997) and Mt. St. Helens (Voight et al., 1981; Janda et al., 1981). Existing drainages within the ring-plain, a network of separate and overlapping, laterally migrating paleo-channels provided flow paths for channelised lahars but were frequently infilled and covered by coarse, voluminous sheet-like flows (c.f. Procter et al., 2009). The tabular debris flow-deposits indicate that they were too large to be contained by the channels. The frequency, nature and volume of the lahars depended on the prevailing local climate, i.e. rainfall intensity and duration in the source region, vegetation patterns and related slope-stability

or sediment supply (e.g. Waitt et al., 1983; Mothes et al., 1998; Hodgson & Manville, 1999; Lavigne et al., 2000; Vallance, 2000; VanWesten & Daag, 2005). Palynological data from the Tepoztlán Formation point to a temperate to humid climate that was strongly affected by the monsoon during the time of deposition (Lenhardt, 2009).

Periods of quiescence or reduced volcanic activity are characterized by reworking and erosion of eruption-related deposits (e.g. Palmer & Walton, 1990), resulting in the deposition of sandy to gravely fluvial deposits. Gravel bars, deposited during these periods, indicate the existence of high-magnitude floods. The development of soils could not be observed. Instead pollen findings in the matrix of the lahars indicate the existence of forest vegetation outside the main active areas (Lenhardt et al., 2008).

Deposition near San Agustín was influenced by a volcanic center relatively close to section SAG itself but now covered by lavas of the Chichinautzin Formation. Paleocurrent data on ignimbrites and dome lavas suggest the volcanic edifice to have lain N to NE of the studied section. The volcanic products are interpreted to come from a lateral parasitic vent at the southeastern flank of the Chichinautzin proto-edifice, which had reached a critical height at this time in terms of slope stability and magma ascent.

In contrast to the central part of the study area around Tepoztlán, the parts to the east (SOM1, SOM2, TON) were not or only partially affected by deposition from the ring-plain system, and show a marginal setting. In particular, the deposition of abundant sheetflood sediments is a sign for floodplain sedimentation in marginal areas of the ring-plain (c.f. Luzón, 2005) or its front, i.e. at the transition to the river system. The dominance of channel-fills and gravel bars indicate a continuation of the braided-river system in these areas, whose fluvial transport is occasionally disrupted by nearby explosive eruptions and abundant pyroclastic material.

Finally, the intrusion of dikes within the Tepoztlán Formation (15.83±1.31 Ma; Lenhardt et al., 2010) is related to a period of plutonic to subvolcanic magma body emplacement and large fissure eruptions that emplaced widespread lava plateaus between the states of Nayarit and Veracruz (Ferrari & Rosas-Elguera, 2000; Ferrari, 2004; Ferrari et al., 2005).

The E-W trending axial braided-river system and also the assumed E-W trending alignment of stratovolcanoes and lava domes within the Tepoztlán Formation can be explained by the existence of the La Pera fault system, existing since pre-Miocene times

(Johnson & Harrison, 1990; Garduno et al., 1993). Studies throughout the TMVB suggest that emplacement of magmatism always occurred in the maximum extensional strain zones (Alaniz-Álvarez et al., 1998; García-Palomo et al., 2000). These zones acted as weakness zones through which the melts could ascend to form the early volcanic arc (Mooser, 1972). In this way, the development of the E-W trending fault system could have significantly influenced the shifting from a N-S to an E-W trending volcanism at the end of the SMO and the initial phase of the TMVB (e.g. Ferrari et al., 1999) through a docking of the magmatic arc volcanism to the newly developed fault system (Lenhardt, 2009).

CONCLUSIONS

Due to excellent outcrops and a set of methods including lithofacies analysis, panel mapping, paleocurrent data and a chronostratigraphic framework it was possible to reconstruct the evolution of an early Miocene volcaniclastic succession at the southern edge of the Transmexican Volcanic Belt (TMVB). The Tepoztlán Formation accumulated mainly in medial to distal settings relative to their source area in flank and apron settings of a volcanic ring plain, which interfingered with an axial W-E trending braided river system. Although a strong interaction of fluvial, eruptive, and gravitational processes, with all kind of transitions, has been observed, a systematic evolution is evident, which is closely related to a complete volcanic cycle of the early TMVB lasting around c. 4 Ma.

In the first phase (Malinalco member, 22.8 - 22.2 Ma), volcanic activity started with a moderate supply of volcanic material erupted from three small stratovolcanoes. Most pyroclastic material could be reworked by sheet floods and fluvial processes along the W-E trending valley. Phase two (San Andres member, 22.2 - 21.3 Ma) records increasing volcanic activity with thick and voluminous pyroclastic flows and lava flows, which temporarily overloaded and buried the fluvial system with debris. Synsedimentary tectonics and pronounced paleorelief show the successive growth of volcanic edifices and possible volcanotectonic events related to major eruptions. During phase three (Tepozteco Member, 21.3 - 18.8 Ma) a large ring plain, mostly composed of mass-flow

deposits, developed at the northeastern edge of the Tepoztlán Formation and prograded over the axial river system. This implies that in early Miocene time a voluminous stratovolcano existed in the area of the present Sierra Chichinautzin, which is now covered by Quaternary lava flows. At this time, it seems that it reached a critical height and steepness, resulting in slope failures and parasitic vent formation. Its altitude must have been at minimum similar to the present day topographic level (c. 3500 m a.s.l.). Marginal settings in the NE show that fluvial processes continued and smaller volcanic centers at lower levels, possibly flank eruptions, became dominant.

Altogether, the Tepoztlán Formation shows a volcanic ring-plain succession with distinct evolutionary steps: initiation with several small volcanic centers (c. 0.6 Ma), build-up of volcanic edifices and paroxysmal eruptions (c. 0.9 Ma), and a destructive period (c. 2.5 Ma) when few big stratovolcanoes were eroded mainly by mass flow processes. This evolution corresponds well to observations from modern volcanic apron settings (e.g. Hacket & Houghton, 1989, Vessel & Davies, 1981, Mack & Rasmussen, 1984, Procter et al., 2009; Zernack et al., 2009) and demonstrates the close connection of ring-plain successions to volcanic cycles.

ACKNOWLEDGEMENTS

This research work is modified from a part of the Doctoral thesis of the first author (Lenhardt, 2009), which was part of a cooperative project between the Technische Universität Darmstadt, Germany and the Universidad Nacional Autónoma de México (UNAM), Mexico. The study was funded by the Deutsche Forschungsgemeinschaft (DFG), project HI 643/5-1. The study greatly benefited from discussions with Peter Schaaf and Claus Siebe at the UNAM, Mexico City. Furthermore, the first author would like to thank Armin Freundt, GEOMAR, Kiel; Fraser Goff, Los Alamos National Laboratory; Cathy Busby, UCSB, and Elena Centeno, UNAM for many helpful discussions at the beginning of the studies for this paper. We are indebted to V. Manville, K. Németh and C. Breitkreuz for their thorough reviews, which significantly helped to improve the quality of the manuscript.

REFERENCES

Alaniz-Álvarez, S.A., Nieto-Samaniego, Á.F. and **Ferrari, L.** (1998) Effect of the strain rate in the distribution of monogenetic and polygenetic volcanism in the Transmexican Volcanic Belt. *Geology*, **26**, 591-594.

Allen, S.R., Stadlbauer, E. and **Keller, J.** (1999) Stratigraphy of the Kos Plateau Tuff: product of a major Quaternary explosive rhyolithic eruption in the eastern Aegean, Greece. *Int. J. Earth. Sci.*, **88**, 132-156.

Arnot, M.J., Good, T.R. and **Lewis, J.J.M.** (1997) Photogeological and image-analysis techniques for collection of large-scale outcrop data. *J. Sediment. Res.*, **67**, 984-987.

Ballance, P.F. (1988) The Huriwai braidplain delta of New Zealand: a late Jurassic, coarsegrained, volcanic-fed depositional system in a Gondwana forearc basin. In: *Fan Deltas: Sedimentology and Tectonic Settings* (Eds. W. Nemec and R.J. Steel), Blackie and Son, Glasgow, 430–444.

Bestland, E. A. (1991) A Miocene Gilbert-type fan-delta from a volcanically influenced lacustrine basin, Rusinga Island, Lake Victoria, Kenya. *J. Geol. Soc. Lond.*, **148(6)**, 1067-1078.

Beverage, J.P. and **Culbertson, J.K.** (1964) Hyperconcentrations of suspended sediment. *Journal of the Hydraulics Division*, Proceedings of the American Association of Civil Engineers, **90**, 117-128.

Blair, T.C. (1987) Tectonic and hydrologic controls on cyclic alluvial fan, fluvial, and lacustrine rift-basin sedimentation, Jurassic – lowermost Cretaceous Todos Santos Formation, Chiapas, Mexico. *J. Sediment. Petrol.*, **57**, 845-862.

Blair, T.C. and **McPherson, J.G.** (1994) Alluvial fans and their natural distinction from rivers based on morphology, hydraulic processes, sedimentary processes, and facies assemblages. *J. Sediment. Res.*, Sect. A 64, 450-489.

Bonnichsen, B. and **Kauffmann, D.F.** (1987) Physical features of rhyolite lava flows in the Snake River Plain volcanic province, south-western Idaho. In: *The emplacement of silicic domes and lava flows* (Ed. J.H. Fink), *Geol. Soc. Am. Spec. Pap.*, **212**, 119-145.

Borgia, A. and **van Wyk de Vries, B.** (2003) The volcano-tectonic evolution of Concepcion, Nicaragua. *Bull. Volcanol.*, **65**, 248–266.

Branney, M.J. and **Kokelaar, P.** (2002) Pyroclastic density currents and the sedimentation of ignimbrites. *Mem. Geol. Soc. Lond.*, **27**, 143 pp.

Bridge, J.S. (1993) The interaction between channel geometry, water flow, sediment transport and deposition in braided rivers. In: *Braided Rivers* (Eds. J.L. Best and C.S. Bristow), *Geol. Soc. Lond. Spec. Publ.*, **75**, 13-71.

Cagnoli, B. and **Tarling, D.H.** (1997) The reliability of anisotropy of magnetic susceptibility (AMS) data as flow direction indicators in friable base surge and ignimbrite deposits: Italian examples. *J. Volcan. Geotherm. Res.*, **75**, 309-320.

Calder, E.S., Luckett, R., Sparks, R.S.J. and **Voight, B.** (2002) Mechanisms of lava dome instability and generation of rockfalls and pyroclastic flows at Soufrière Hills Volcano, Montserrat. In: *The Eruption of Soufrière Hills Volcano, Montserrat, from 1995 to 1999* (Eds. T.H. Druitt and B.P. Kokelaar), *Geol. Soc. Lond. Mem.*, **21**, 173-190.

Cañón-Tapia, E. and **Castro, J.** (2004) AMS measurements on obsidian from the Inyo Domes, CA: a cpmparison of magnetic and mineral preferred orientation fabrics. *J. Volcanol. Geotherm. Res.*, **134**, 169-182.

Cantagrel, J. and **Robin, C.** (1979) K-Ar dating on eastern Mexican volcanic rocks – Relations between the andesitic and alkaline provinces. *J. Volcanol. Geotherm. Res.*, **5**, 99-114.

Capra, L. and **Macías, J.L.** (2000) Pleistocene cohesive debris flows at Nevado de Toluca Volcano, central Mexico. *J. Volcanol. Geotherm. Res.*, **102**, 149-167.

Capra, L., Macías, J. and **Garduno, V.** (1997) The Zitácuaro Volcanic Complex, Michoacán, México: Magmatic and eruptive history of a resurgent caldera. *Geofísica Internacional*, **36(3)**, 161-179.

Capra, L., Macías, J.L., Scott, K.M., Abrams, M. and **Garduno-Monroy, V.H.** (2002) Debris avalanches and debris flows transformed from collapses in the Trans-Mexican Volcanic Belt, Mexico – Behavior and implications for hazard assessment. *J. Volcanol. Geotherm. Res.*, **113**, 81-110.

Carey, S. (2000) Volcaniclastic sedimentation around island arcs. In: *Encyclopedia of volcanoes* (Ed. H. Sigurdsson), Academic Press, San Diego, 627–642.

Carey, S.N. and **Sigurdsson, H.** (1989) The intensity of Plinian eruptions. *Bull. Volcanol.*, **51**, 28-40.

Carrasco-Núnez, G. (1999) Holocene block-and-ash flows from summit dome activity of Citlaltépetl volcano, Eastern Mexico. *J. Volcanol. Geotherm. Res.*, **88**, 47–66.

Carrasco-Núnez, G., Milán, M. and **Verma, S.** (1989) Geología del volcán El Zamorano, Estado de Querétaro. *Revista Instituto de Geología*, **8**, 194-201.

Carrasco-Núnez, G., Gómez-Tuena, A. and **Lorenzo-Velázquez, L.** (1997) Geologic map of Cerro Grande Volcano and surrounding area, central Mexico: *Geol. Soc. Am. Map and Chart Series*, **MCH081**, 1-10.

Cas, R.A.F. and **Wright, J.V.** (1987) Volcanic successions – modern an ancient. Allen & Unwin, London, 528 pp.

Chamyal, L.S., Khadkikar, A.S., Malik, J.N. and **Maurya, D.M.** (1997) Sedimentology of the Narmada alluvial fan, western India. *Sediment. Geol.*, 107, 263-279.

Clemente, P. and **Perez-Arlucea, M.** (1993) Depositional architecture of Cuerda del Pozo Formation, Lower Cretaceous of the extensional Cameros basin, north-central Spain. *J. of Sed. Petrol.*, **63**, 437-452.

Cole, R.B. and **DeCelles, P.G.** (1991) Subaerial to submarine transitions in early Miocene pyroclastic flow deposits, southern San Joaquin basin, California. *Geol. Soc. Am. Bull.*, **103**, 221-235.

Collinson, J.D. (1996) Alluvial sediments. In: *Sedimentary Environments: Processes, Facies and Stratigraphy* (Ed. H.G. Reading), pp. 37-82, Blackwell, Oxford.

Coussot, P. and **Meunier, M.** (1996) Recognition, classification and mechanical description of debris flows. *Earth-Sci. Rev.*, **40**, 209-227.

Cronin, S.J. and **Neall, V.E.** (1997) A late Quaternary stratigraphic framework for the northeastern Ruapehu and eastern Tongariro ring plains, New Zealand. *N.Z. J. Geol. Geophys.*, **40**, 185-197.

Cronin, S.J., Neall, V.E. and **Palmer, A.S.** (1996) Geological history of the northeastern ring plain of Ruapehu volcano, New Zealand. *Quat. Int.*, **35**, 21–28.

Davidson, J.P. and **De Silva, S. (**2000) Composite volcanoes. In: *Encyclopedia of Volcanoes* (Eds. H. Sigurdsson, B. Houghton, S. McNutt, H. Rymer and J. Stix), Academic Press, San Diego, 663–681.

De Cserna, Z. and **Fries, C.** (1981a) Hoja Taxco 14 Q-h (7), con resumen de la geología de la hoja Taxco, estados de Guerrero, México y Morelos: Universidad Autónoma de México, Instituto de Geología, Carta Geológica de México, Serie 1:100 000, map with text, 47 pp.

De Cserna, Z. and **Fries, C.** (1981b) The Volcanic Centre of Zempoala, Central-Mexico. *Geofísica Internacional*, **34**, 98-117.

Demant, A. (1978) Características del Eje Neovolcánico Transmexicano y sus problemas de interpretacíon. *Revista Instituto de Geología*, **2**, 172-187.

Donoghue, S.L. and **Neall, V.E.** (2001) Late Quaternary constructional history of the southeastern Ruapehu ring plain, New Zealand. *N.Z. J. Geol. Geophys.*, **44**, 439–466.

Einsele, G. (2000): Sedimentary Basins. Evolution, Facies, and sediment Budget. 2nd edn., Springer Verlag, Heidelberg, Berlin, New York, 792 pp.

Ferrari, L. (2004) Slab detachment control on mafic volcanic pulse and mantle heterogeneity in central Mexico. *Geology*, **32(1)**, 77-80.

Ferrari, L. and **Rosas-Elguera, J.** (2000) Late Miocene to Quaternary extension at the northern boundary of the Jalisco block, western Mexico: The Tepic-Zacoalco rift revised. In: *Cenozoic Tectonics and Volcanism of Mexico* (Eds. G. Aguirre-Díaz, H. Delgado-Granados and J. Stock), *Geol. Soc. Am. Spec. Pap.*, **334**, 42-64.

Ferrari, L., Lopez-Martinez, M., Aguirre-Díaz, G. and **Carrasco-Núñez, G.** (1999) Space-time patterns of Cenozoic arc volcanism in Central Mexico: From the Sierra Madre Occidental to the Mexican volcanic belt. *Geology*, **27**, 303-306.

Ferrari, L., Vaggelli, G., Petrone, C., Manetti, P. and **Conticelli, S.** (2000) Late Miocene volcanism and intra-arc tectonics during the early development of the Trans-Mexican Volcanic Belt. *Tectonophysics*, **318**, 161-185.

Ferrari, L., López-Martínez, M., González-Cervantes, N., Jacobo-Albarrán, J. and **Hernández-Bernal, M.** (2003) Volcanic record and age of formation of the Mexico City basin. *Reunión Annual de la Unión Geofísica Mexicana*, **23**, 120.

Ferrari. L., Tagami, T., Eguchi, M., Orozco-Esquivel, M., Petrone, C., Jacobo-Albarrán, J. and **López-Martínez, M.** (2005) Geology, geochronology and tectonic setting of late Cenozoic volcanism along the southwestern Gulf of Mexico: The Eastern Alkaline Province revisited. *J. Volcanol. Geotherm. Res.*, **146**, 284-306.

Ferrucci, M., Pertusati, S., Sulpizio, R., Zanchetta, G., Pareschi, M.T. and **Santacroce, R.** (2005) Volcaniclastic debris flows at La Fossa Volcano (Vulcano Island, southern Italy): Insights for erosion behaviour of loose pyroclastic material on steep slopes. *J. Volcanol. Geotherm. Res.,* **145**, 173-191

Fisher, R.V. (1961) Proposed classification of volcaniclastic sediments and rocks. *Bull. Geol. Soc. Am.*, **72**, 1409-1414.

Fisher, R.V. and **Schminke, H.U.** (1984) Pyroclastic Rocks. Springer-Verlag, Berlin. 472 pp.

Fisher, R.V., Orsi, G., Ort, M. and **Heiken G.** (1993) Mobility of a large-volume pyroclastic flow - emplacement of the Campanian ignimbrite, Italy. *J. Volcanol. Geotherm. Res.,* **56**, 205-220.

Francis, P.W. (1994) Volcanoes: A Planetary Perspective. Oxford University Press, Oxford, 443 pp.

Freundt, A. and **Schmincke, H.-U.** (1995) Eruption and emplacement of a basaltic welded ignimbrite during caldera formation on Gran Canaria. *Bull. Volcanol.*, **56**, 640-659.

Freundt, A., Wilson, C.J.N. and **Carey, S.N.** (2000) Ignimbrites and block-and ash flow deposits. In: *Encyclopedia of volcanoes* (Eds. H. Sigurdsson, B. Houghton, S.R. McNutt, H. Rymer and J. Stix), Academic, San Diego, 581-599.

Fries, C. (1960) Geología del Estado de Morelos y de partes adyacentes de México y Guerrero, región central meridional de México. *Boletín del Instituto Geología*, UNAM, **60**, 1-236.

García-Palomo, A. (1998) Evolucion estructural en las inmediaciones del Volcan Nevado de Toluca, Edo. De Mexico. [unpublished] M.Sc. thesis, Universidad Autónoma de México, Instituto de Geología, Mexico, 146 pp.

García-Palomo, A., Macías, J.L. and **Garduno, V.H.** (2000) Miocene to recent structural evolution of the Nevado de Toluca volcano region, Central Mexico. *Tectonophysics*, **318**, 281-302.

García-Palomo, A., Macías, J.L., Arce, J.L., Capra, L., Garduño, V.H. and **Espíndola, J.M.** (2002) Geology of Nevado de Toluca Volcano and surrounding areas, central Mexico. Boulder, Colorado, *Geol. Soc. Am. Map and Chart Series*, **MCH089**, 1-26.

Garduno, V.H., Spinnler, J. and **Ceragioli, E.** (1993) Geological and structural study of the Chapala Rift, state of Jalisco, Mexico. *Geofísica Internacional*, **32**, 487-499.

Geißler, M., Breitkreuz, C. and **Kiersnowski H.** (2008) Late Paleozoic volcanism in the central part of the Southern Permian Basin (NE Germany, W Poland): facies distribution and volcano-topographic hiati. *Int. J. Earth Sci.*, **97**, 973–989.

Gómez-Tuena, A. and **Carrasco-Núnez, G.** (2000) Cerro Grande Volcano: The evolution of a Miocene stratocone in the early Transmexican Volcanic Belt. *Tectonophysics*, **318**, 249-280.

Gómez-Tuena, A., LaGatta, A., Langmuir, C., Goldstein, S., Ortega-Gutiérrez, F. and **Carrasco-Núnez, G.** (2003) Temporal control of subduction magmatism in the Eastern Trans-Mexican Volcanic Belt: Mantle sources, slab contributions and crustal contamination. *Geochem., Geophys., Geosyst.*, **4**, 8912, doi:10.1029/2003GC000524.

Gómez-Tuena, A., Orozco-Esquivel, Ma.T. and **Ferrari, L.** (2007) Igneous petrogenesis of the Trans-Mexican Volcanic Belt. In: *Geology of México - Celebrating the Centenary of the Geological Society of México* (Eds. S.A. Alaniz-Álvarez and Á.F. Nieto-Samaniego), *Geol. Soc. Am. Spec. Pap.*, **422**, 129-181.

Hackett, W.R. and **Houghton, B.F.** (1989) A facies model for a quaternary andesitic composite volcano: Ruapehu, New Zealand. *Bull. Volcanol.*, **51**, 51-68.

Hampton, M.A. (1975) Competence of fine-grained debris flows. *J. Sediment. Petrol.*, **45**, 834-844.

Harms, J.C., Southard, J.B., Spearing, D.R. and **Walker, R.G.** (1982) Depositional environments as interpreted from primary sedimentary structures and stratification sequences. Lecture Notes, Soc. Econ. Paleontol. Mineral., Short Course 2, Dallas, 161 pp.

Hodgson, K.A. and **Manville, V.R.** (1999) Sedimentology and flow behaviour of a raintriggered lahar, Mangatoetoenui Stream, Ruapehu volcano, New Zealand. *Bull. Geol. Soc. Am.*, **111**, 743–754.

Horton, B.K. and **DeCelles, P.G.** (2001) Modern and ancient fluvial megafans in the foreland basin system of the central Andes, southern Bolivia: implications for drainage network evolution in fold-thrust belts. *Basin Research*, **13**, 43-63.

Hoshizumi, H., Uto, K. and **Watanabe, K.** (1999) Geology and eruptive history of Unzen volcano, Shimabara Peninsula, Kyushu, SW Japan. *J. Volcanol. Geotherm. Res.*, **89**, 81–94.

Janda, R.J., Scott, K.M., Nolan, K.M. and **Martinson, H.A.** (1981) Lahar movement, effects, and deposits. In: *The 1980 eruptions of Mount St. Helens,Washington* (Eds. P.W. Lipman and D.R. Mullineaux), *U.S. Geol. Survey Prof. Pap.*, **1250**, 461–478.

Jo, H.R., Rhee, C.W. and **Chough, S.K.** (1997) Distinctive characteristics of a streamflow-dominated alluvial fan deposit: Sanghori area, Kyongsang Basin (Early Cretaceous), southeastern Korea. *Sed. Geol.*, **110**, 51-79.

Johnson, C. and **Harrison, C.** (1990) Neotectonics in central Mexico. *Phy. Earth Planet. In.*, **64**, 187-210.

Johnson, A.M. and **Rodine, J.R.** (1984) Debris Flow. In: *Slope Instability* (Eds. D. Brunsden and D.B. Prior), pp. 257-361, Wiley, Chichester.

Karátson, D. and **Nemeth, K.** (2001) Lithofacies associations of an emerging volcaniclastic apron in a Miocene volcanic complex: an example from the Börzsöny Mountains, Hungary. *Int. J. Earth. Sci.*, **90**, 776-794.

Kataoka, K. (2005) Distal fluvio-lacustrine volcaniclastic resedimentation in response to an explosive silicic eruption: The Pliocene Mushono tephra bed, Central Japan. *Geol. Soc. Am. Bull.*, **117(1/2)**, 3-17.

Kataoka, K.S., Manville, V., Nakajo T. and **Urabe A.** (2009) Impacts of explosive volcanism on distal alluvial sedimentation: Examples from the Pliocene—Holocene volcaniclastic successions of Japan. *Sed. Geol.*, 220, 306-317.

Kostic, B., Süss, M.P. and **Aigner, T.** (2007) Three-dimensional sedimentary architecture of Quaternary sand and gravel resources: a case study of economic sedimentology (SW Germany). *Int. J. Earth Sci.*, **96**, 743-767.

Kuenzi, W.D., Horst, O.H. and **McGehee, R.V.** (1979) Effect of volcanic activity on fluvial-deltaic sedimentation in a modern arc-trench gap, southwestern Guatemala. *Bull. Geol. Soc. Am.*, **90**, 827-838.

Kuhnle, R.A. (1996) Unsteady transport of sand and gravel mixtures. In: *Advances in Fluvial Dynamics and Stratigraphy* (Eds. P.A. Carling and M.R. Dawson), pp. 183-202, Wiley, West Sussex, England.

Lavigne, F., Thouret, J.-C., Voight, B., Suwa, H. and **Sumaryono, A.** (2000) Lahars at Merapi volcano, Central Java: an overview. *J. Volcanol. Geotherm. Res.*, **100**, 423–456.

Lenhardt, N. (2009) Volcaniclastic successions of the southern edge of the Transmexican Volcanic Belt: evidence for the Miocene plate reorganisation in Central America (Morelos, Mexico). PhD Thesis, Darmstadt University of Technology, 141 pp. Available at: http://tuprints.ulb.tu-darmstadt.de/1405/.

Lenhardt, N., Herrmann, M., Mosbrugger, V. and **Hinderer, M.** (2008) Palynology of the Tepoztlán Formation, Central Mexico – palaeoenvironmental and

palaeoclimatological implications. *Terra Nostra 2008/2*, 12th International Palynological Congress IPC-XII/IOPC-VIII, Bonn, Abstract Volume, p. 162.

Lenhardt, N., Böhnel, H., Wemmer, K., Torres-Alvarado, I.S., Hornung, J. and **Hinderer, M.** (2010) Petrology, magnetostratigraphy and geochronology of the Miocene volcaniclastic Tepoztlán Formation: implications for the initiation of the Transmexican Volcanic Belt (Central Mexico). *Bull. Volcanol.*, **72**, 817-832. doi: 10.1007/s0045-010-0361-z.

Lock, B.E. (1978) Ultrahigh-temperature volcanic mudflows amongst the Drakensberg volcanic rocks: New criteria for their recognition. *Trans. Geol. Soc. S. Afr.*, **81**, 55-59.

López-Infanzón, M. (1991) Petrologic study of the volcanic rocks in the Chiconquiaco-Palma Sola area, central Veracruz, Mexico. [unpublished] M.Sc. thesis, New Orleans, Tulane University, pp. 1-139.

Luzón, A. (2005) Oligocene-Miocene alluvial sedimentation in the northern Ebro Basin, NE Spain: Tectonic control and palaeogeographical evolution. *Sed. Geol.*, **177**, 19-39.

MacDonald, G.A. (1972) Volcanoes. Prentice-Hall, Engelwood Cliffs, NJ, 510 pp.

Mack, G.H. and **Rasmussen, K.A.** (1984) Alluvial-fan sedimentation of the Cutler Formation (Permo-Pennsylvanian) near Gateway, Colorado. *Bull. Geol. Soc. Am.*, **95**, 109-116.

Manville, V.R. (2001) Sedimentology and history of Lake Reporoa: an ephemeral supra-ignimbrite lake, Taupo Volcanic Zone, New Zealand. In: *Volcanogenic sedimentation in lacustrine settings* (Eds. J.D.L. White and N.R. Riggs), *Int. Ass. Sediment. Spec. Publ.*, **30**, 109-140.

Manville, V. (2002) Sedimentary and geomorphic responses to a large ignimbrite eruption: readjustment of the Waikato River in the aftermath of the A.D. 181 Taupo eruption, New Zealand. *J. Geol.*, **110**, 519-542.

Manville, V., Segschneider, B. and **White, J.D.L.** (2002) Hydrodynamic behaviour of Taupo 1800a pumice: implications for the sedimentology of remobilised pyroclastic deposits. *Sedimentology*, **49**, 955–976.

Manville, V., Németh, K. and **Kano, K.** (2009) Source to sink: A review of three decades of progress in the understanding of volcaniclastic processes, deposits, and hazards. *Sed. Geol.*, **220**, 136-161.

Márquez, A., Verma, S., Anguita, F., Oyarzun, R. and **Brandle, J.** (1999) Tectonics and volcanism of Sierra Chichinautzin: Extension at the front of the central transmexican volcanic belt. *J. Volcanol. Geotherm. Res.*, **93**, 125-150.

Mathisen, M.E. and **Vondra, C.F.** (1983) The fluvial and pyroclastic deposits of the Cagayan Basin, Northern Luzon, Philippines-an example of non-marine volcaniclastic sedimentation in an interarc basin. *Sedimentology*, **30**, 369-392.

McPhie, J., Doyle, M. and **Allen, R.** (1993) Volcanic textures – a guide to the interpretation of textures in volcanic rocks. Centre for Ore Deposit and Exploration Studies, University of Tasmania, 198 pp.

Miall, A.D. (1977) A review of the braided river depositional environment. *Earth Sci. Rev.*, **13**, 1-62.

Miall, A.D. (1978) Lithofacies types and vertical profile models in braided rivers: a summary. *Can. Soc. Pet. Geol. Mem.*, **5**, 597–604.

Miall, A.D. (1985) Architectural-element analysis: a new method of facies analysis applied to fluvial deposits. *Earth Sci. Rev.*, **22**, 261-308.

Miall, A.D. (1996) The Geology of Fluvial Deposits. Springer-Verlag, Berlin, 581 pp.

Mooser, F. (1972) The Mexican volcanic belt structure and tectonics. *Geofís. Intl.*, **12**, 55-70.

Mothes, P.A., Hall, M.L. and **Janda, R.J.** (1998) The enormous Chillos Valley Lahar: an ash-flow generated debris flow from Cotopaxi Volcano, Ecuador. *Bull. Volcanol.*, **59**, 233–244.

Mueller, W. (1991) Volcanism and related slope to shallow marine volcaniclastic sedimentation: an Archean example Chibougamau, Quebec, Canada. *Precamb. Res.*, **49**, 1-22.

Negendank, J., Emmermann, R., Krawczyk, R., Mooser, F., Tobschall, H. and **Wehrle, D.** (1985) Geological and geochemical investigations on the eastern Trans-Mexican Volcanic Belt. *Geofís. Intl.*, **24**, 477-575.

Nemec, W. and **Postma, G.** (1993) Quaternary alluvial fans in southwestern Crete: sedimentation processes and geomorphic evolution. In: *Alluvial sedimentation* (Eds. M. Marzo and C. Puigdefábregas), *Int. Ass. Sediment. Spec. Publ.*, **17**, 235-276.

Németh. K. (2001) Deltaic density currents and turbidity deposits related to maar crater rims and their importance for palaeogeographic reconstruction of the Bakony-Balaton Highland Volcanic Field, Hungary. In: *Particulate gravity currents* (Eds. W.D. McCaffrey, B.C. Kneller and J. Peakall), *Int. Ass. Sediment. Spec. Publ.*, **31**, 261-277.

Nixon, G., Demant, A., Armstrong, R. and **Harakal, J.** (1987) K-Ar and geologic data bearing on the age and evolution of the Trans-Mexican Volcanic Belt. *Geofís. Intl.*, **26**, 109-158.

Ochoterena, H. (1978) Origen y edad del Tepozteco. *Boletin del Instituto de Geografía*, **8**, 41-54.

Orozco-Esquivel, M., Petrone, C., Ferrari, L., Tagami, T. and **Manetti, P.** (2007) Geochemical and isotopic variability controlled by slab detachment in a subduction zone with varying dip: The eastern Trans-Mexican Volcanic Belt. *Lithos*, **93**, 149-174.

Orton, G.J. (1996) Volcanic environments. In: *Sedimentary Environments: Processes, Facies and Stratigraphy Reading* (Eds. H.G. Reading), pp. 485-567, Blackwell Science, Oxford.

Palmer, B.A. (1991) Holocene lahar deposits in the Whakapapa catchment, northwestern ring plain, Ruapehu volcano (North Island, New Zealand). *N.Z. J. Geol. Geophys.*, **34**, 177–190.

Palmer, B.A. and **Neall, V.E.** (1991) Contrasting lithofacies architecture in ring-plain deposits related to edifice construction and destruction, the Quaternary Stratford and Opunake Formations, Egmont Volcano, New Zealand. *Sed. Geol.*, **74**, 71-88.

Palmer, B.A. and **Walton, A.W.** (1990) Accumulation of volcaniclastic aprons in the Mount Dutton Formation (Oligocene-Miocene), Marysvale volcanic field, Utah. *Bull. Geol. Soc. Am.*, **102**, 734-748.

Palmer, B.A., Purves, A.M. and **Donoghue, S.L.** (1993) Controls on accumulation of a volcaniclastic fan, Ruapehu composite volcano, New Zealand. *Bull. Volcanol.*, **55**, 176-189.

Pasquaré, G., Ferrari, L., Garduño, V., Tibaldi, A. and **Vezzoli, L.** (1991) Geology of the central sector of the Mexican Volcani Belt, States of Guanajuato and Michoacan. *Geol. Soc. Am. Maps and Charts Series*, **MCH072**, scale 1:300,000, 1 sheet, 22 pp.

Pérez-Venzor, J., Aranda-Gómez, J., McDowell, F. and **Solorio Munguía, J.** (1996) Geología del Volcán Palo Huérfano, Guanajuato, México. *Rev. Mex. Cienc. Geol.*, **13**, 174-183.

Pierson, T.C. (1997) Hydrologic consequences of hot-rock/snowpack interactions at Mount St. Helens volcano, Washington, 1982-84. *U.S. Geological Survey Open-file report*, **96-179**, 115 pp.

Pierson, T.C. (2005) Hyperconcentrated flow – transitional process between water flow and debris flow. In: *Debris-flow Hazards and Related Phenomena* (Eds. M. Jakob and O. Hunger), pp. 159-202, Springer Praxis Books, Springer, Heidelberg.

Pierson, T.C. and **Scott, K.M.** (1985) Downstream dilution of lahars: transition from debris flow to hyperconcentrated streamflow. *Water Resour. Res.*, **21,** 1511-1524.

Pierson, T.C., Daag, A.S., Reyes, P.J.D., Regalado, M.T.M., Solidum, R.U. and **Tubianosa, B.S.** (1996) Flow and deposition of post-eruption hot lahars on the east side of Mount Pinatubo, July-October 1991. In: *Fire and Mud, Eruptions and Lahars of Mount Pinatubo, Philippines* (Eds. C.G. Newhall and R.S. Punongbayan), pp. 921-950, Philippines Institute of Volcanology and Seismology, Univ. Washington Press.

Platz, T., Cronin, S.J., Cashman, K.V., Stewart, R.B. and **Smith, I.E.M.** (2007) Transitions from effusive to explosive phases in andesite eruptions – a case-study from the AD 1655 eruption of Mt. Taranaki, New Zealand. *J. Volcanol. Geotherm. Res.*, **161**, 15–34.

Procter, J.N., Cronin, S.J. and **Zernack, A.V.** (2009) Landscape and sedimentary response to catastrophic debris avalanches, western Taranaki, New Zealand. *Sed. Geol.*, **220**, 271–287.

Reid, I. and **Frostick, L.E.** (1987) Towards a better understanding of bedload transport. In: *Recent Developments in Fluvial Sedimentology* (Eds. F.G. Etheridge, R.M. Flores and M.D. Harvey), *Spec. Publ.-Soc Econ. Paleontol. Mineral.*, Tulsa, **39**, 13-20.

Riggs, N.R. and **Busby-Spera, C.J.** (1990) Evolution of a multi-vent volcanic complex within a subsiding arc graben depression: Mount Wrightson Formation, Arizona. *Bull. Geol. Soc. Am.*, **102**, 1114–1135.

Riggs, N.R. and **Busby-Spera, C.J.** (1991) Facies analysis of an ancient, dismembered, large caldera complex and implications for intra-arc subsidence: Middle Jurassic strata of Cobre Ridge, southern Arizona, USA. *Sed. Geol.*, **74**, 39–68.

Riggs, N. and **Carrasco-Núnez, G.** (2004) Evolution of a complex isolated dome system, Cerro Pizarro, central México. *Bull. Volcanol.*, **66**, 322-335.

Robin, C., Eissen, J.-P. and **Monzier, M.** (1994) Ignimbrites of basaltic andesite and andesite compositions from Tanna, New Hebrides Arc. *Bull. Volcanol.*, **56**, 10-22.

Rodolfo, K.S. and **Arguden, A.T.** (1991) Rain-lahar generation and sediment-delivery systems at Mayon volcano, Philippines, In: *Sedimentation in Volcanic Settings* (Ed. R.V. Fisher and G.A. Smith), *Spec. Publ. Soc. Econ. Paleont. Miner.*, **45**, 71-87.

Rose, W.I., Self, S., Murrow, P.J., Bonadonna, C., Durant, A.J. and **Ernst, G.G.J.** (2008) Nature and significance of small volume fall deposits at composite volcanoes: Insights from the October 14, 1974 Fuego eruption, Guatemala. *Bull. Volcanol.*, **70**, 1043-1067.

Ross, C.S. and **Smith, R.L.** (1961) Ash-flow tuffs. Their origin, Geological Relations and Identification. *U.S. Geol. Survey Prof. Pap.*, **366**, 81 pp.

Rowley, P.D., Kuntz, M.A. and **MacLeod, N.S.** (1981) Pyroclastic flow deposits. In: *The 1980 Eruptions of Mount St. Helens, Washington* (Eds. P.W Lipmann and D.R. Mullineaux), *U.S. Geol. Surv. Prof. Pap.*, **1250**, 489-512.

Runkel, A.C. (1990) Lateral and temporal changes in volcanogenic sedimentation; analysis of two Eocene sedimentary aprons, Big Bend region, Texas. *J. Sed. Petrol.*, **60**, 747-760.

Schneider, J.-L., Le Ruyet, A., Chanier, F., Buret, C., Ferrière, J., Proust, J.-N. and **Rosseel, J.-B.** (2001) Primary or secondary distal volcaniclastic turbidites: how to make the distinction? An example from the Miocene of New Zealand (Mahia Peninsula, North Island). *Sed. Geol.*, **145**, 1-22.

Scott, K.M. (1985) Lahars and Lahar-runout Flows in the Toutle-Cowlitz River system, Mount St. Helens, Washington — Origins, Behavior, and Sedimentology. *U.S. Geol. Survey Open-File Report*, **85-500**, 202 pp.

Segschneider, B., Landis, C.A., Manville, V., White, J.D.L. and **Wilson, C.J.N.** (2002) Environmental response to a large, explosive rhyolite eruption: sedimentology of post-1.8 ka pumice-rich Taupo volcaniclastics in the Hawke's Bay region, New Zealand. *Sed. Geol.*, **150**, 275–299.

Sheth, H.C., Torres-Alvarado, I. and **Verma, S.** (2000) Beyond subduction and plumes: A unified tectonic-petrogenic model for the Mexican volcanic belt. *International Geology Review*, **42**, 1116-1132.

Siebe, C. and **Macías, J.L.** (2004) Volcanic hazards in the Mexico City metropolitan area from eruptions at Popocatépetl, Nevado de Toluca, and Jocotitlán stratovolcanoes

and monogenetic scoria cones in the Sierra Chichinautzin Volcanic Field. Penrose Field Guide: Penrose Field Guide 1, 77 pp.

Siebe, C., Abrams, M. and **Sheridan, M.F.** (1991) Holocene age of a major block-and-ash-flow fan at the western slopes of Pico de Orizaba volcano. Convención sobre la evolución geológica de México. Memoria, Pachuca, Hidalgo, 203-204.

Siebe, C., Abrams, M. and **Sheridan, M.F.** (1993) Major Holocene block-and-ash fan at the western slope of ice-capped Pico de Orizaba volcano, México: Implications for future hazards. *J. Volcanol. Geotherm. Res.*, **59**, 1-33.

Siebe, C., Rodríguez-Lara, V., Schaaf, P. and **Abrams, M.** (2004) Geochemistry, Sr-Nd isotope composition, and tectonic setting of Holocene Pelado, Guespalapa and Chichinautzin scoria cones, south of Mexico City. *J. Volcanol. Geotherm. Res.*, **130(3-4)**, 197-226

Siegenthaler, C. and **Huggenberger, P.** (1993) Pleistocene Rhine gravel: deposits of a braided river system with dominant pool preservation. In: *Braided Rivers* (Eds. J.L. Best and C.S. Bristow), *Geol. Soc. Spec. Publ.*, **75**, 147-162.

Smith, G.A. (1986) Coarse-grained volcaniclastic sediment: termindology and depositional process. *Bull. Geol. Soc. Am.*, **97**, 1-10.

Smith, G.A. (1987) The influence of explosive volacanism on fluvial sedimentation: the Deschutes Formation (Neogene) in central Oregon. *J. Sediment. Petrol.*, **57**, 613-629.

Smith, G.A. (1988) Sedimentology of proximal to distal volcaniclastics dispersed across an active foldbelt: Ellensburg Formation (late Miocene), central Washington. *Sedimentology*, **35**, 953-977.

Smith, S.A. (1990) The sedimentology and accretionary style of an ancient gravel-bed stream: the Budleigh Salterton Pebble Beds (Lower Triassic), southwest England. *Sed. Geol.*, **67**, 199-219.

Smith, G.A. (1991) Facies sequences and geometries in continental volcaniclastic sediments. In: *Sedimentation in Volcanic Settings* (Eds. R.V. Fisher and G.A. Smith), *SEPM Spec. Publ.*, **45**, 1-257.

Smith, G.A. and **Landis, C.A.** (1995) Intra-arc basins. In: *Tectonics of sedimentary basins* (Eds. C.J. Busby and R.V. Ingersoll), pp. 263-298, Blackwell Science Inc., Boston.

Smith, G.A. and **Lowe, D.R.** (1991) Lahars: volcano-hydrologic events and deposition in the debris flow – hyperconcentrated flow continuum. In: *Sedimentation in Volcanic Settings* (Eds. R.V. Fisher and G.A. Smith, G.A.), *Soc. Econ. Paleontol. Mineral., Spec. Publ.*, **45**, 59-70.

Sohn, Y.K., Rhee, C.W. and **Kim, B.C.** (1999) Debris flow and hyperconcentrated flood-flow deposits in an alluvial fan, northwestern part of the Cretaceous Yongdong Basin, Central Korea. *J. Geol.*, **107**, 111-132.

Sparks, R.S.J. (1976) Grain size variations in ignimbrites and implications for the transport of pyroclastic flows. *Sedimentology*, **23**, 147-188.

Stach, E., Mackowsky, M.T., Teichmüller, M., Taylor, G.H. and **Chandra, D.** (1982): Stach's Textbook of Coal Petrology. Borntraeger, Berlin, 535 pp.

Steel, R.J. and **Thompson, D.B.** (1983) Structures and textures in Triassic braided stream conglomerates (‘Bunter’ Pebble Beds) in the Sherwood Sandstone Group, North Staffordshire, England. *Sedimentology*, **30**, 341-367.

Todd, S.P. (1996) Process deduction from fluvial sedimentary structures. In: *Advances in Fluvial Dynamics and Stratigraphy* (Eds. P.A. Carling and M.R. Dawson) pp. 299-350, Wiley, Chichester.

Trauth, N. (2007) Aufschlusswandkartierung, Lithofazies- und Architekturelement-analyse in der vulkanoklastischen Formacíon Tepoztlán, Zentral Mexiko. [unpublished] student research project, Institute of Applied Geosciences, Darmstadt University of Technology, 53 pp.

Uba, C.J., Heubeck, C. and **Hulka, C.** (2005) Facies analysis and basin architecture of the Neogene Subandean synorogenic wedge, southern Bolivia. *Sed. Geol.*, **180**, 91-123.

Ui, T., Matsuwo, N., Sumita, M. and **Fujinawa, A.** (1999) Generation of block and ash flows during the 1990-1995 eruption of Unzen Volcano, Japan. *J. Volcanol. Geotherm. Res.*, **80**, 123-137.

Valdéz-Moreno, G., Aguirre-Díaz, G. and **López-Martínez, M.** (1998) El Volcán La Joya, Edos. De Querétaro y Guanajuato. Un estratovolcán antiguo del cinturón volcánico mexicano. *Rev. Mex. Cienc. Geol.*, **15**, 181-197.

Valentine, G.A. (1987) Stratified flow in pyroclastic surges. *Bull. Volcanol.*, **49**, 616-630.

Vallance, J.W. (2000) Lahars. In: *Encyclopedia of Volcanoes* (Eds. H. Sigurdsson, B. Houghton, S. McNutt, H. Rymer and J. Stix), pp. 601–616, Academic Press.

Vallance, J.W. and **Scott, K.M.** (1997) The Osceola Mudflow from Mount Rainier; sedimentology and hazard implications of a huge clay-rich debris flow. *Bull. Geol. Soc. Am.*, **109**, 143–163.

VanWesten, C.J. and **Daag, A.S.** (2005) Analysing the relation between rainfall characteristics and lahar activity at Mount Pinatubo, Philippines. *Earth Surface Processes and Landforms*, **30**, 1663–1674.

Verma, S. (1999) Geochemistry of evolved magmas and their relationship to subduction-unrelated mafic volcanism at the volcanic front of the central Mexican Volcanic Belt. *J. Volcanol. Geotherm. Res.*, **93**, 151-171.

Verma, S. (2000) Geochemistry of the subducting Cocos plate and the origin of subduction-unrelated mafic volcanism at the front of the central Mexican Volcanic Belt. In: *Cenozoic Tectonics and Volcanism of Mexico* (Eds. H. Delgado-Granados, G. Aguirre-Díaz and J. Stock), *Geol. Soc. Am. Spec. Pap.*, **334**, 1-28.

Verma, S. (2002) Absence of Cocos plate subduction-related basic volcanism in southern Mexico: A unique case on Earth? *Geology*, **30**, 1095-1098.

Verma, S. and **Carrasco-Núnez, G.** (2003) Reappraisal of the geology and geochemistry of Volcán Zamorano, Central Mexico: Implications for the discrimination of the Sierra Madre Occidental and Mexican Volcanic Belt province. *Int. Geol. Rev.*, **45**, 724-752.

Vessel, R.D. and **Davies, D.K.** (1981) Nonmarine sedimentation in an active fore arc basin. In: *Nonmarine Depositional Environments: Models for Exploration* (Eds. F.G. Ethridge and R.M. Flores). *Soc. Econ. Paleontol. Mineral. Spec. Publ.*, **31**, 34-45.

Voight, B., Glicken, H., Janda, R.J. and **Douglass, P.M.** (1981) Catastrophic rockslide avalanche of May 18. In: *The 1980 eruptions of Mount St. Helens, Washington* (Eds. P.W. Lipman and D.R. Mullineaux), *U.S. Geol. Survey Prof. Pap.*, **1250**, 347–377.

Waitt Jr., R.B., Pierson, T.C., MacLeod, N.S., Janda, R.J., Voight, B. and **Holcomb, R.T.** (1983) Eruption-triggered avalanche, flood and lahar at Mount St. Helens: effects of winter snowpack. *Science*, **22**, 1394–1397.

Walker, R.G. and **Cant, D.J.** (1984) Sandy fluvial systems. In: *Facies Models* (Ed. R.G. Walker), 2nd edition, *Geoscience Canada Reprint Series*, **1**, 71-89.

Walton, A.W. and **Palmer, B.A.** (1988) Lahar facies of the Mount Dutton Formation (Oligocene-Miocene) in the Marysvale volcanic field, Utah. *Bull. Geol. Soc. Am.*, **100**, 1078-1091

White, J.D.L. and **Busby-Spera, C.J.** (1987) Deep marine arc apron deposits and syndepositional magmatism in the Alisitos Group at Punta Cono, Baja California, Mexico. *Sedimentology*, **34**, 911-928.

White, J.D.L. and **Houghton, B.F.** (2006) Primary volcaniclastic rocks. *Bull. Geol. Soc. Am.*, **34**, 677-680.

White, J.D.L. and **Robinson, P.T.** (1992) Intra-arc sedimentation in a low-lying marginal arc, Eocene Clarno Formation, central Oregon. *Sed. Geol.*, **80**, 89-114.

Whitham, A.G. (1989) The behaviour of subaerially produced pyroclastic flows in a subaqueous environment: evidence from the Roseau eruption, Dominica, West Indies. *Mar. Geol.*, **86**, 27-40.

Whiting, P.J., Dietrich, W.E., Leopold, L.B., Drake, T.G. and **Shereve, R.L.** (1988) Bedload sheets in heterogeneous sediment. *Geology*, **16**, 105-108.

Williams, H. and **McBirney, A.R.** (1979) Volcanology. Freeman and Cooper, San Francisco, Calif., 391 pp.

Wilson, C.J.N. and **Walker, G.P.L.** (1982): Ignimbrite depositional facies: the anatomy of a pyroclastic flow. *J. Geol. Soc. Lond.*, **139**, 581-592.

Wizevich, M.C. (1991) Photomosaics of outcrops: useful photographic techniques. In: *The three-dimensional facies architecture of terrigenous clastic sediments and its implications for hydrocarbon discovery and recovery* (Eds. A.D. Miall and N. Tyler), *Concepts in Sedimentology and Paleontology*, **3**, SEPM, Tulsa, OK, 22-24.

Wright, J.V., Smith, A.L. and **Self, S.** (1980) A working terminology of pyroclastic deposits. *J. Volcanol. Geotherm. Res.*, **8**, 315-336.

Xin, R., Li, G., Feng, Z., Liang, J. and **Lin, C.** (2009) Depositional characteristics of lake-floor fan of cretaceous lower Yaojia Formation in western part of central depression region, Songliao basin. *J. Earth Sci.*, **20(4)**, 731-745

Zanella, E., De Astis, G., Dellino, P., Lanza, R. and **La Volpe, L.** (1999) Magnetic fabric and remanent magnetization of pyroclastic surge deposits from Vulcano (Aeolian Islands, Italy). *J. Volcanol. Geotherm. Res.*, **93**, 217–233.

Zernack, A.V., Procter, J.N. and **Cronin, S.J.** (2009) Sedimentary signatures of cyclic growth and destruction of stratovolcanoes: A case study from Mt. Taranaki, New Zealand. *Sed. Geol.*, **220**, 288–305.